Chikako Kamae, MD[a]
Noriko Nakagawa, MD, PhD[a]
Hiroki Sato, MS[b]
Kenichi Honma, MD[a]
Noriko Mitsuiki, MD[c,d]
Osamu Ohara, PhD[c]
Hirokazu Kanegane, MD, PhD[e]
Srdjan Pasic, MD, PhD[f]
Qiang Pan-Hammarström, MD, PhD[g]
Menno C. van Zelm, PhD[h]
Tomohiro Morio, MD, PhD[d]
Kohsuke Imai, MD, PhD[a]
Shigeaki Nonoyama, MD, PhD[a]

From the Departments of [a]Pediatrics and [b]Preventive Medicine and Public Health, National Defense Medical College, Saitama, Japan; [c]the Department of Human Genome Research, Kazusa DNA Research Institute, Chiba, Japan; [d]the Department of Pediatrics, Tokyo Medical and Dental University, Tokyo, Japan; [e]the Department of Pediatrics, University of Toyama, Toyama, Japan; [f]the Department of Immunology, Mother and Child Health Institute, Medical Faculty, University of Belgrade, Belgrade, Serbia; [g]the Department of Laboratory Medicine, Karolinska Institute, Karolinska University Hospital, Huddinge, Stockholm, Sweden; and [h]the Department of Immunology, Erasmus MC, University Medical Center, Rotterdam, The Netherlands. E-mail: kimai.ped@tmd.ac.jp.

Supported in part by grants from the Ministry of Defense; the Ministry of Health, Labour, and Welfare; and the Ministry of Education, Culture, Sports, Science, and Technology.

Disclosure of potential conflict of interest: The authors declare that they have no relevant conflicts of interest.

REFERENCES

1. Yong PFK, Thaventhiran JED, Grimbacher B. "A rose is a rose is a rose," but CVID is not CVID. common variable immune deficiency (CVID), what do we know in 2011? Adv Immunol 2011;111:47-107.
2. Resnick ES, Moshier EL, Godbold JH, Cunningham-Rundles C. Morbidity and mortality in common variable immune deficiency over 4 decades. Blood 2012;119: 1650-7.
3. Moratto D, Gulino AV, Fontana S, Mori L, Pirovano S, Soresina A, et al. Combined decrease of defined B and T cell subsets in a group of common variable immunodeficiency patients. Clin Immunol 2006;121:203-14.
4. Chapel H, Lucas M, Lee M, Bjorkander J, Webster D, Grimbacher B, et al. Common variable immunodeficiency disorders: division into distinct clinical phenotypes. Blood 2008;112:277-86.
5. Morinishi Y, Imai K, Nakagawa N, Sato H, Horiuchi K, Ohtsuka Y, et al. Identification of severe combined immunodeficiency by T-cell receptor excision circles quantification using neonatal Guthrie cards. J Pediatr 2009;155:829-33.
6. Nakagawa N, Imai K, Kanegane H, Sato H, Yamada M, Kondoh K, et al. Quantification of κ-deleting recombination excision circles in Guthrie cards for the identification of early B-cell maturation defects. J Allergy Clin Immunol 2011;128:223-5.e2.
7. van Zelm MC, Szczepanski T, Van Der Burg M, Van Dongen JJM. Replication history of B lymphocytes reveals homeostatic proliferation and extensive antigen-induced B cell expansion. J Exp Med 2007;204:645-55.
8. Verbsky JW, Baker MW, Grossman WJ, Hintermeyer M, Dasu T, Bonacci B, et al. Newborn screening for severe combined immunodeficiency; the Wisconsin experience (2008-2011). J Clin Immunol 2012;32:82-8.
9. Rizzi M, Neumann C, Fielding AK, Marks R, Goldacker S, Thaventhiran J, et al. Outcome of allogeneic stem cell transplantation in adults with common variable immunodeficiency. J Allergy Clin Immunol 2011;128:1371-2.

Available online December 28, 2012.
http://dx.doi.org/10.1016/j.jaci.2012.10.059

Homing frequency of human T cells inferred from peripheral blood depletion kinetics after sphingosine-1-phosphate receptor blockade

To the Editor:

Naive and central memory (CM) T cells home through lymph nodes (LNs), whereas T cells with an effector memory (EM) phenotype preferentially screen peripheral tissues in search of cognate antigen.[1] LN entry and egress are distinct and highly regulated processes mediated by an orchestrated interplay of chemokines/chemokine receptors and adhesion molecules.[2] Interaction of peripheral node addressins with L-selectin on T cells allows tethering/rolling along high endothelial venules (HEVs).[2] Interaction of the chemokine receptor CCR7 with its ligands CCL19/CCL21 and CXCR4 with CXCL12 then mediates firm adhesion to HEVs through high-affinity interactions of lymphocyte function–associated antigen 1 and intercellular adhesion molecule 1, permitting transmigration of T cells across the HEV cell layer.[2] Within the LNs, T-cell migration is directed through T-cell zones toward the cortical sinuses.[3] A sphingosine-1-phosphate (S1P) gradient established across the endothelial cells of the cortical sinuses is directing LN egress of T cells through efferent lymph back to the peripheral blood circulation.[4] Acting as a functional antagonist on the S1P receptor, the pharmacologic compound fingolimod, which has shown efficacy in the treatment of multiple sclerosis (MS), blocks this egress.[4,5] As a consequence, in fingolimod-treated subjects naive and CM T cells are trapped in LNs and reduced in the blood circulation.[6]

Here, by studying depletion kinetics of T cells in the blood of *de novo* fingolimod-exposed subjects in combination with *in vitro* migration experiments, homing frequencies and LN access hierarchy between T-cell subsets were derived indirectly. First, we defined the effect of *de novo* fingolimod exposure on the number of circulating $CD4^+$ and $CD8^+$ phenotypic T-cell subsets in patients with MS during a 6-hour observation period (hourly measurements, 1 time before and 6 times after drug exposure) by using flow cytometry (detailed information on patients and methods is provided in the Methods section and Table E1 in this article's Online Repository at www.jacionline.org). In fingolimod-treated subjects, 6 hours after the first drug dose, numbers of $CD4^+$ T-cell subsets with an LN homing phenotype (ie, naive and CM T cells) were significantly reduced (Fig 1, *A* [representative example; absolute cell counts], and Fig 1, *B* [pooled data; proportional change]). Intriguingly, the kinetics of reduction differed between phenotypic naive (CD62 ligand [CD62L]–positive $CD45RA^+$) and CM ($CD62L^+CD45RA^-$) $CD4^+$ T cells. Specifically, compared with baseline measurements, naive $CD4^+$ T-cell counts started to decrease earlier than CM $CD4^+$ T-cell counts (2 vs 5 hours after fingolimod exposure; Fig 1, *B*). In $CD8^+$ T cells, contrasting $CD4^+$ T cells, only naive ($CD62L^+CD45RA^+$) $CD8^+$ T-cell counts decreased significantly (after 3 vs 2 hours in naive $CD4^+$ T cells) after the first dose of fingolimod (Fig 1, *C* [representative example; absolute cell counts], and Fig 1, *D* [pooled data; proportional change]).

On the basis of these *ex vivo* depletion kinetics, *in vitro* chemotaxis experiments were performed, as described in the Methods section in this article's Online Repository. In a transwell system spontaneous migration of bulk $CD4^+$ and $CD8^+$ T cells was comparably low in healthy control subjects and untreated patients with MS (and was further decreased in the presence of fingolimod; see Fig E1 in this article's Online Repository at www.jacionline.org). Gradients of CXCL12, CCL19, and CCL21 mediated a clear increase in migration of bulk $CD4^+$ and $CD8^+$ T cells from healthy control subjects and untreated patients with MS, which was not significantly influenced by fingolimod (see Fig E1). Dot plot distribution (as a percentage) of migrated versus nonmigrated, phenotypic naive, CM, EM, and (for $CD8^+$ T cells) CD45RA re-expressing EM cells (EMRA) was then compared between control cells (spontaneous migration) and cells that migrated toward CXCL12, CCL19, or CCL21. An example of CXCL12-mediated changes in the

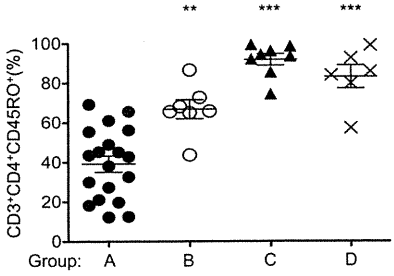

FIG E1. $CD45RO^+CD3^+CD4^+$ T-cell frequency within $CD4^+CD3^+$ lymphocytes was analyzed among groups. $CD45RO^+CD3^+CD4^+$ lymphocyte counts were significantly higher in groups B, C, and D compared with those in group A ($P < .0001$). Group A: 37% ± 16%; group B: 67% ± 13% (**$P < .01$); group C: 92% ± 8.2% (***$P < .001$); and group D: 83% ± 14% (***$P < .001$).

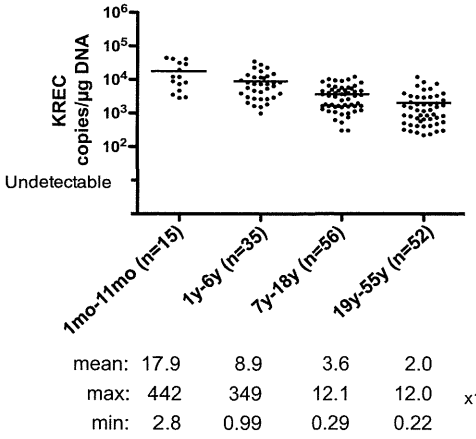

mean:	17.9	8.9	3.6	2.0
max:	442	349	12.1	12.0
min:	2.8	0.99	0.29	0.22

x10^3 copies/µg DNA

FIG E2. KREC levels were analyzed in genomic DNA samples extracted from peripheral blood of control subjects at different age groups (n = 158; age range, 1 month to 55 years). KREC levels were significantly higher in infants (17.9 ± 3.9 × 10^3 copies/µg DNA) compared with other children's age groups (8.9 ± 1.3 × 10^3 copies/µg DNA in the 1- to 6-year-old group and 3.6 ± 3.8 × 10^3 copies/µg DNA in the 7- to 18-year-old group) and adults (2.0 ± 3.3 × 10^3 copies/µg DNA; $P < .0001$).

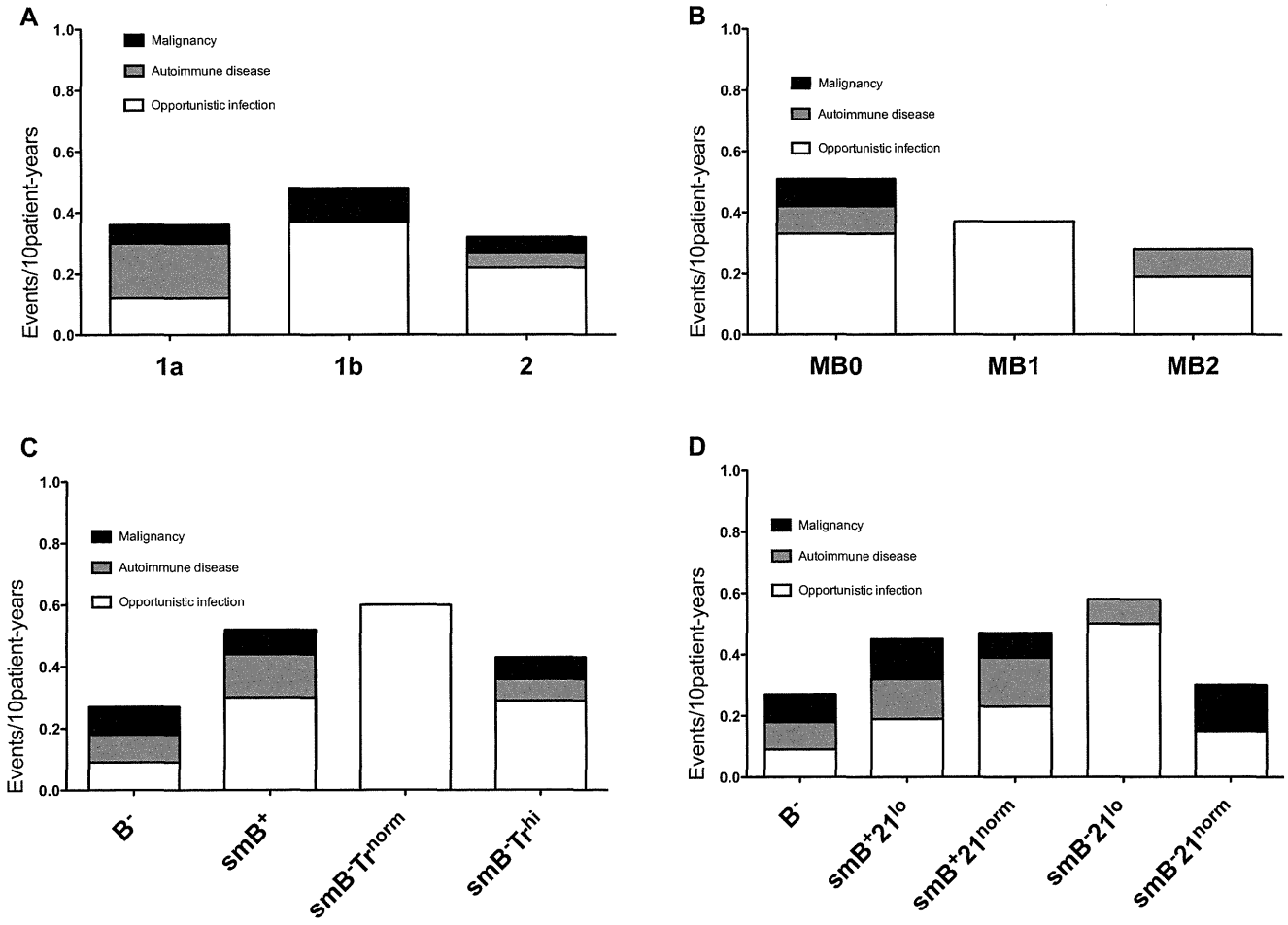

FIG E3. Patients were classified in the following way and analyzed for cumulative incidence of complications: **A,** Freiburg; **B,** Paris; and **C,** EUROclass classifications, according to $CD38^{hi}IgM^{hi}$ transitional B cells (Fig E3, *A-C*) or $CD21^{low}$ B cells **(D)**. Five patients were excluded from the Freiburg and Paris classifications because of decreased B-cell numbers (<1%). Additionally, we excluded 4 patients in the Freiburg classification, 1 patient in the Paris classification, and 4 patients in the EUROclass classification for transitional B cells and 8 in the EUROclass classification for $CD21^{low}$ B cells because of lack of data. The following cumulative events/10 patient-years were found. Freiburg classification: 1a, 0.36; 1b, 0.48; 2, 0.32. Paris classification: MB0, 0.50; MB1, 0.37; MB2, 0.28. EUROclass classification according to transitional B cells: B^-, 0.27; smB^+, 0.52; smB^-Tr^{norm}, 0.60; smB^-Tr^{high}, 0.43. EUROclass classification according to $CD21^{lo}$ B cells: B^-, 0.27; smB^+21^{lo}, 0.45; smB^+21^{norm}, 0.47; smB^-21^{lo}, 0.58; smB^-21^{norm}, 0.30. No classification showed any significantly increased events in any particular group according to calculated *P* values, as follows—Freiburg classification: 1a vs 2 = .898, 1b vs 2 = .479, 1a vs 1b = .838; Paris classification: MB0 vs MB2 = .179, MB1 vs MB2 = .654, MB0 vs MB1 = .764; EUROclass classification according to transitional B cells: B^- vs smB^+ = .298, smB^-Tr^{norm} vs smB^+ = .809, smB^-Tr^{hi} vs smB^+ = .702, smB^-Tr^{hi} vs smB^-Tr^{norm} = .641, smB^-Tr^{norm} vs B^- = .329, smB^-Tr^{hi} vs B^- = .508; EUROclass classification according to $CD21^{lo}$ B cells: B^- vs smB^+21^{norm} = .443, smB^+21^{lo} vs smB^+21^{norm} = .930, smB^-21^{lo} vs smB^+21^{norm} = .695, smB^-21^{norm} vs smB^+21^{norm} = .575, B^- vs smB^-21^{norm} = .926, smB^+21^{lo} vs smB^-21^{norm} = .609, smB^-21^{lo} vs smB^-21^{norm} = .399, B^- vs smB^+21^{lo} = 0.474, B^- vs smB^-21^{lo} = 0.270, smB^+21^{lo} vs smB^-21^{lo} = 0.618.

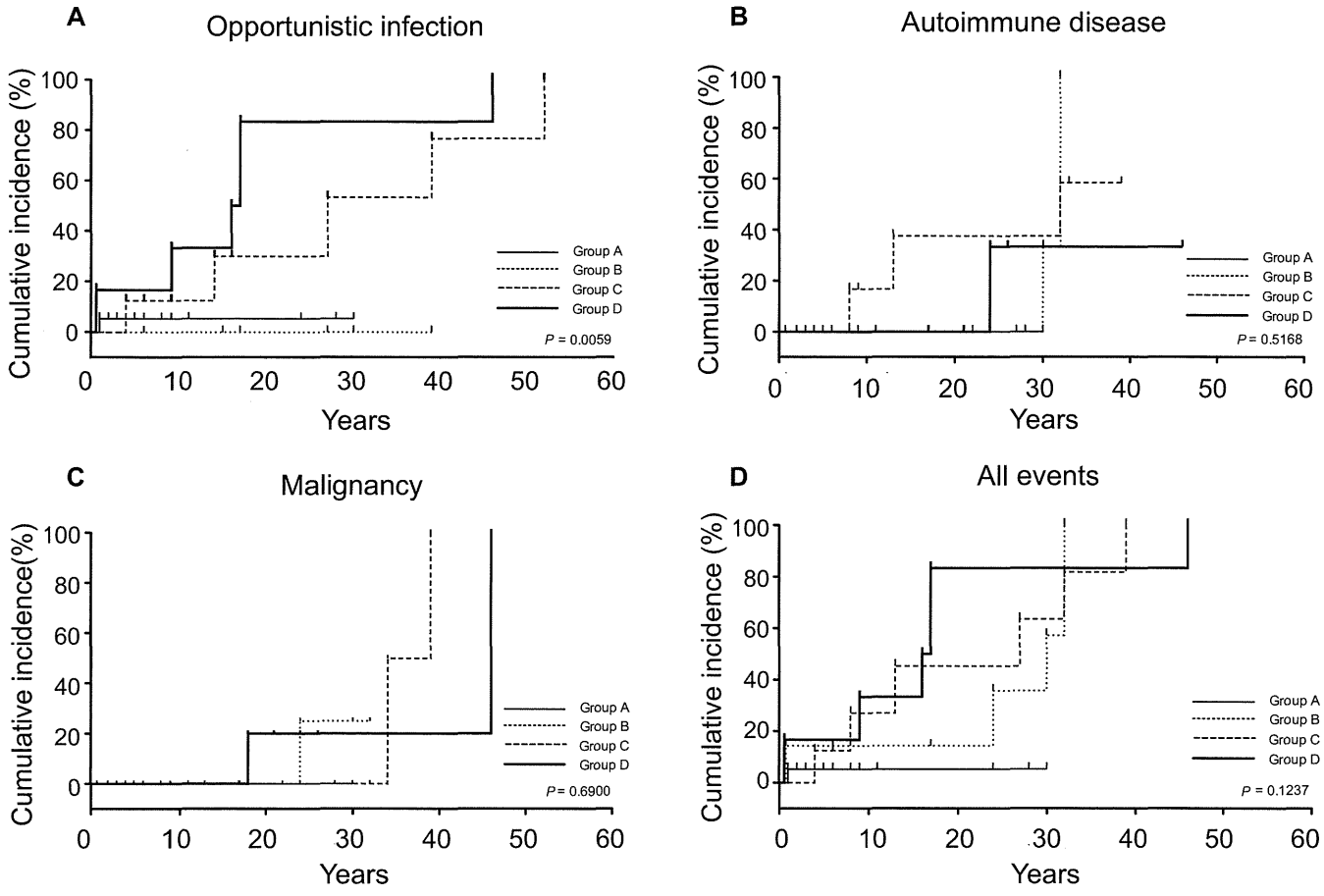

FIG E4. Comparing longitudinal cumulative incidence of complication events among groups. Cumulative incidence was estimated separately and longitudinally by using the Kaplan-Meier method and statistically compared between groups by using the log-rank test. The cumulative incidence of opportunistic infections **(A)**, autoimmune diseases **(B)**, malignancies **(C)**, and all events **(D)** is shown.

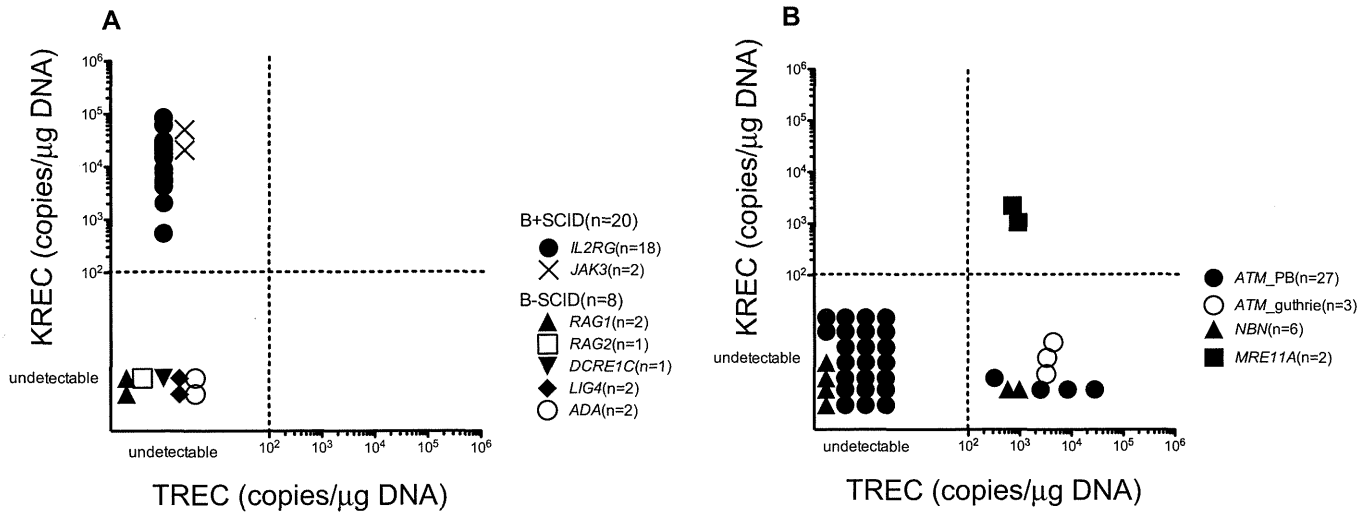

FIG E5. TREC and KREC quantification classifies patients with SCID, AT, NBS, or ataxia-telangiectasia–like disease *(ATLD)* into 4 groups. **A,** Patients with B^+SCID (n = 20) were classified as group C, and patients with B^-SCID (n = 8) were classified as group D; these patients were included in the previous studies.[5,6] **B,** Although most patients with AT (n = 23) and patients with NBS (n = 4) were classified as group D, TRECs were detected in peripheral blood samples (n = 4 in patients with AT and n = 2 in patients with NBS) and neonatal Guthrie cards (n = 3) of some patients with AT, who were classified as group B. Patients with ATLD with *MRE11A* mutations were classified as group A.

T-cell receptor ligation causes Wiskott-Aldrich syndrome protein degradation and F-actin assembly downregulation

Yuko Watanabe, MD, PhD,[a]* Yoji Sasahara, MD, PhD,[a]* Narayanaswamy Ramesh, PhD,[b]* Michel J. Massaad, PhD,[b]* Chung Yeng Looi, PhD,[a] Satoru Kumaki, MD, PhD,[a] Shigeo Kure, MD, PhD,[a] Raif S. Geha, MD,[b]‡ and Shigeru Tsuchiya, MD, PhD[a]‡ *Miyagi, Japan, and Boston, Mass*

Background: Wiskott-Aldrich syndrome protein (WASP) links T-cell receptor (TCR) signaling to the actin cytoskeleton. WASP is normally protected from degradation by the Ca^{++}-dependent protease calpain and by the proteasome because of its interaction with the WASP-interacting protein.
Objective: We investigated whether WASP is degraded after TCR ligation and whether its degradation downregulates F-actin assembly caused by TCR ligation.
Methods: Primary T cells, Jurkat T cells, and transfected 293T cells were used in immunoprecipitation experiments. Intracellular F-actin content was measured in splenic T cells from wild-type, WASP-deficient, and c–Casitas B-lineage lymphoma (Cbl)-b–deficient mice by using flow cytometry. Calpeptin and MG-132 were used to inhibit calpain and the proteasome, respectively.
Results: A fraction of WASP in T cells was degraded by calpain and by the ubiquitin-proteasome pathway after TCR ligation. The Cbl-b and c-Cbl E3 ubiquitin ligases associated with WASP after TCR signaling and caused its ubiquitination. Inhibition of calpain and lack of Cbl-b resulted in a significantly more sustained increase in F-actin content after TCR ligation in wild-type T cells but not in WASP-deficient T cells.
Conclusion: TCR ligation causes WASP to be degraded by calpain and to be ubiquitinated by Cbl family E3 ligases, which targets it for destruction by the proteasome. WASP degradation might provide a mechanism for regulating WASP-dependent TCR-driven assembly of F-actin. (J Allergy Clin Immunol 2013;132:648-55.)

Key words: *Wiskott-Aldrich syndrome, Wiskott-Aldrich syndrome protein, T-cell receptor, calpain, ubiquitination, proteasome, F-actin, Cbl family proteins*

Abbreviations used
Arp: Actin-related protein
Cbl: Casitas B-lineage lymphoma
EVH1: Ena-VASP homology domain 1
IS: Immune synapse
TCR: T-cell receptor
WAS: Wiskott-Aldrich syndrome
WASP: Wiskott-Aldrich syndrome protein
WIP: WASP-interacting protein
WT: Wild-type
ZAP-70: ζ Chain–associated protein kinase of 70 kDa

Wiskott-Aldrich syndrome (WAS) is an X-linked recessive disorder characterized by variable immunodeficiency, eczema, and thrombocytopenia.[1] The gene for Wiskott-Aldrich syndrome protein (WASP) is mutated in patients with WAS and X-linked thrombocytopenia. *WAS* is located on Xp11.22-p11.23 and encodes a protein of 502 amino acids and approximately 60 kDa in molecular weight.[2,3] WASP expression is restricted to hematopoietic cells.[3]

WASP has an N-terminal Ena/VASP homology domain 1 (EVH1) domain, a Cdc42/Rac GTPase-binding domain, a proline-rich domain, a G actin–binding verprolin homology (V) domain, a cofilin homology (C) domain, and a C-terminal acidic (A) segment.[1] The last 3 domains are located at the C-terminal end of WASP and are collectively referred to as the VCA domain. WASP interacts with WASP-interacting protein (WIP) through its EVH1 domain; with Cdc42-GTP through its GTPase-binding domain; with multiple SH3 domain–containing proteins, which include Nck, Grb2, and cortactin, through its proline-rich region; and with the actin-related protein (Arp) 2/3 complex that initiates actin polymerization through its VCA domain.[4-6]

WASP plays a critical role in T-cell activation and actin reorganization.[7-9] T cells from patients with WAS and $WASP^{-/-}$ mice are deficient in their ability to increase their F-actin content, secrete IL-2, and proliferate after T-cell receptor (TCR) ligation.[10-12] WASP exists in cells in a closed inactive conformation through intramolecular interactions that prevent the VCA domain from activating the Arp2/3 complex. Binding of Cdc42-GTP or of the SH3 domain of adaptor proteins, as well as phosphorylation of tyrosine (Y) at position 291, is thought to cause a conformational change in WASP, which allows the VCA domain to interact with and activate the Arp2/3 complex.[5,13-15] The WASP-interacting protein (WIP) is expressed at high levels in lymphoid tissues. Most of WASP is associated with WIP in T cells.[16] WIP binds through its C-terminal end to the EVH1 domain of WASP. WIP plays an important role in the recruitment of the WASP-WIP complex to ζ chain–associated protein kinase of 70 kDa (ZAP-70) and

From [a]the Department of Pediatrics, Tohoku University Graduate School of Medicine, Miyagi, and [b]the Division of Immunology, Children's Hospital, and the Department of Pediatrics, Harvard Medical School, Boston.
*These authors contributed equally to this work.
‡These authors contributed equally as senior authors.
Supported by grants-in-aid from the Japan Ministry of Education, Culture, Sports, Science and Technology and a grant for research on intractable diseases from the Japan Ministry of Health, Labour and Welfare (to Y.S. and S.T.), grants from the Japan Foundation for Pediatric Research and the Mother and Child Health Foundation (to Y.S.) and by US Public Health Service grant HL059561.
Disclosure of potential conflict of interest: The authors have been supported by one or more grants from the National Institutes of Health.
Received for publication January 9, 2013; revised March 28, 2013; accepted for publication March 29, 2013.
Available online May 16, 2013.
Corresponding author: Yoji Sasahara, MD, PhD, Department of Pediatrics, Tohoku University Graduate School of Medicine, 1-1 Seiryo-machi, Aoba-ku, Sendai, Miyagi 980-8574, Japan. E-mail: ysasahara@med.tohoku.ac.jp.
0091-6749/$36.00

http://dx.doi.org/10.1016/j.jaci.2013.03.046

to the immunologic synapse after TCR ligation.[17] More importantly, WIP stabilizes WASP in T cells. This is evidenced by the finding that WASP levels are significantly reduced in T cells from $WIP^{-/-}$ mice and a WIP-deficient patient.[16,18] Furthermore, most missense mutations in WASP that result in diminished WASP levels are localized to the WIP-binding EVH1 domain of WASP and disrupt the WASP-WIP interaction.[19,20] Expression of the WASP-binding domain of WIP in these cells restores WASP levels close to normal.[21] Treatment with calpain and proteasome inhibitors increases WASP protein levels in T cells from $WIP^{-/-}$ mice and patients with WAS with missense mutations that disrupt WIP binding,[16] indicating that WASP can be subject to degradation by calpain and the ubiquitin-proteasome pathway.

Unregulated activation of WASP is detrimental to many cell types, especially cells of the myeloid lineage. Three different mutations of WASP, namely L270P, S272P, and I294T, destroy the autoinhibitory conformation of WASP, resulting in a constitutively active protein, and cause X-linked neutropenia.[22] The L270P and S272P mutations localize to the GTPase-binding domain,[23] whereas the I294T mutation is located close to the tyrosine residue Y291, which, when phosphorylated, results in the activation of WASP.[24] Knock-in mouse models mimicking the L270P and I294T mutations have been described.[25] T and B cells from these mice show a marked increase in F-actin levels but migrate normally in response to chemokines.

In this study we demonstrate that TCR ligation causes WASP to be degraded by calpain and by Casitas B-lineage lymphoma (Cbl)–mediated ubiquitination and proteasomal destruction. We demonstrate that WASP degradation provides a mechanism for downregulating TCR-driven assembly of F-actin.

METHODS

Cell lines and T cells

Jurkat T cells were obtained from the American Type Culture Collection and maintained in RPMI medium (Gibco, Carlsbad, Calif) supplemented with 10% FBS. 293T cells were a gift from Dr N. Ishii (Tohoku University, Sendai, Japan) and were maintained in Dulbecco modified Eagle medium (Gibco) supplemented with 10% FBS. Spleens from Cbl-b knockout (*Cbl-b*$^{-/-}$) mice and genetically matched wild-type (WT) shipping controls were a generous gift from Dr H. Gu, Columbia University. WASP-deficient mice were obtained from Dr Scott Snapper. Splenic T cells were isolated by using T-cell enrichment columns (Miltenyi Biotec, Bergisch Gladbach, Germany).

Antibodies

Anti-WASP 5A5 mAb, which recognizes the epitope in the region corresponding to amino acids 146 to 265, was developed in our laboratory.[26] Anti-WASP rabbit polyclonal antibody K374 (a gift from Dr Ignacio Molina) is directed to the C-terminal 20 amino acids of WASP.[16] Anti–phospho-WASP antibody, which recognized WASP phosphorylated on Y291, was purchased from Abcam (Cambridge, United Kingdom). Anti-ubiquitin mAb P4D1, anti–c-Cbl mAb A-9, and anti–Cbl-b mAb G-1 were from Santa Cruz Biotechnology (Santa Cruz, Calif). Anti-actin mAb and anti-FLAG mAb were from Sigma (St Louis, Mo). Anti-HA mAb was from Cell signaling (Danvers, Mass). Control rabbit IgG was from Upstate (Billerica, Mass).

TCR stimulation, immunoprecipitation, and Western blotting

TCR ligation was performed, as described previously.[17] Briefly, T cells were incubated with 10 μg/mL anti-CD3 mAb UCHT1 (Calbiochem, San Diego, Calif) on ice for 20 minutes, followed by cross-linking with 15 μg/mL goat anti-mouse IgG (H+L; Caltag, Buckingham, United Kingdom) at 37°C for the indicated period. Cells were lysed in ice-cold lysis buffer containing 1% Triton X-100 and protease inhibitors. Cell lysates were clarified at 14,000*g* for 20 minutes at 4°C. For immunoprecipitation, cell lysates were precleared with protein G–Sepharose (GE Healthcare, Fairfield, Conn) for 2 hours and incubated overnight at 4°C with 4 μg of the indicated antibody preadsorbed onto protein G–Sepharose. Beads were washed 4 times with modified lysis buffer containing 0.2% Triton X-100. Bound proteins were eluted, run on 10% SDS-PAGE gels, and analyzed by means of Western blotting with the indicated antibodies followed by anti-mouse or anti-rabbit antibodies conjugated to horseradish peroxidase and enhanced chemiluminescent detection (Amersham Life Sciences, Piscataway, NJ). Densitometry was performed with CS Analyzer version 2.08 software (ATTO Corporation, Tokyo, Japan) or ImageJ version 1.45 software.

Calpain and proteasome inhibition

The proteasome inhibitor MG132 and the calpain inhibitor calpeptin were purchased from Calbiochem. Cells were cultured with calpeptin (1 μmol/L) or MG132 (10 μmol/L) for 6 hours before anti-CD3 stimulation.

Expression vectors and transfection

Human pcDNA3.1-EGFP-hWASP-WT was a generous gift from Dr K. A. Siminovitch (University of Toronto, Toronto, Ontario, Canada). Control pAcGFP1-C1 vector was purchased from Clontech (Mountain View, Calif). Human pcDNA3.1-3xFLAG-c-Cbl-WT, pcDNA3.1-3xFLAG-Cbl-b-WT, and pcDNA3.1-HA-Ub were gifts from Drs N. Ishii and Y. Tanaka (Tohoku University).[27] Control p3xFLAG-CMV-14 vector was purchased from Sigma. 293T cells were transiently transfected with lipofectamine, as described previously,[27] and harvested 48 hours after transfection.

Determination of cellular F-actin content

Flow cytometric analysis of F-actin content was performed, as described previously.[16] Briefly, mouse T cells were purified by using negative selection with the Pan T Cell Isolation Kit (Miltenyi Biotec) and then incubated for 6 hours with 1 μmol/L calpeptin. Cells were then washed and incubated with 10 μg/mL rat anti-mouse CD3 mAb (Serotec, Oxford, United Kingdom) for 30 minutes on ice. Cells were stimulated for the indicated times by cross-linking with goat anti-rat IgG (H+L) secondary antibody (Jackson Immunoresearch, West Grove, Pa). Cells were fixed in 4% formaldehyde, washed, and permeabilized with the CytoFix/CytoPerm cell staining kit (BD Biosciences, San Jose, Calif). F-actin was stained with tetramethylrhodamine isothiocyanate–labeled phalloidin (Invitrogen, Carlsbad, Calif). F-actin content was analyzed by measuring the mean fluorescent intensity with FACS LSRFortessa (Becton Dickinson) and FlowJo (TreeStar, Ashland, Ore) software.

Statistical analysis

Statistical analysis was performed with the Student *t* test.

RESULTS

WASP is C-terminally truncated by calpain after TCR ligation

Purified peripheral blood T cells were stimulated with anti-CD3 mAb followed by cross-linking with secondary antibody and cell lysates were immunoblotted for WASP to investigate whether WASP is degraded after TCR ligation. Immunoblotting with mAb 5A5, which recognizes an epitope in the region corresponding to amino acids 146 to 265, revealed a 62- to 64-kDa band in unstimulated T cells (Fig 1, *A*), as previously observed.[28] Stimulation with anti-CD3 resulted in the appearance of a 55-kDa

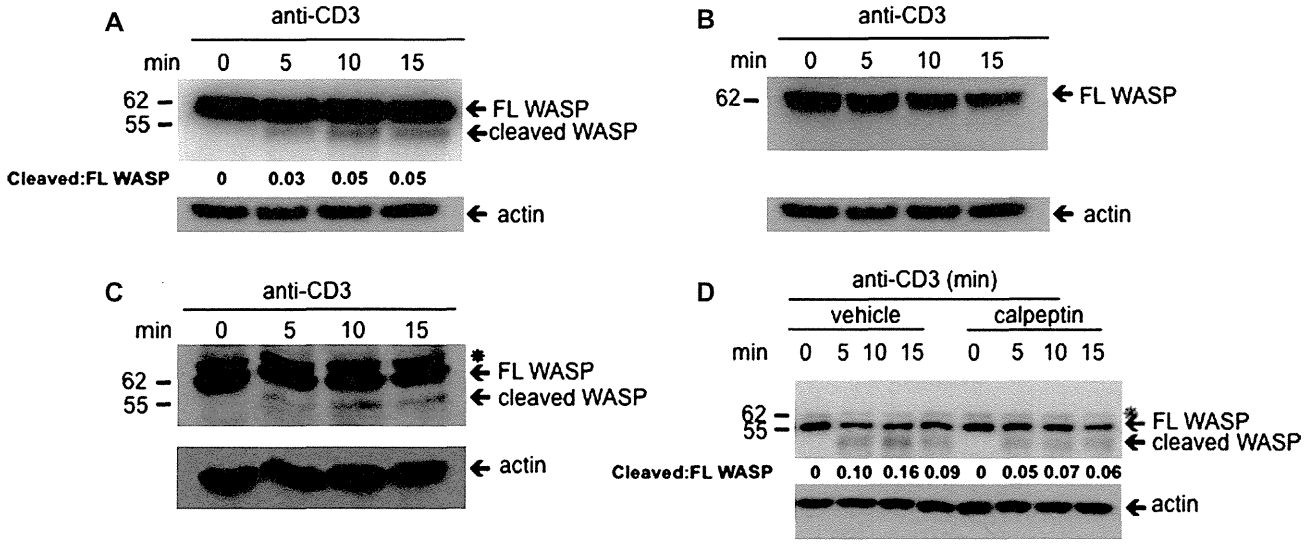

FIG 1. WASP is cleaved by calpain after TCR ligation. **A** and **B**, WASP immunoblot of peripheral blood T cells stimulated for 0 to 15 minutes with anti-CD3 mAb using mAb 5A5 (Fig 1, *A*) or polyclonal antibody K374 (Fig 1, *B*). **C**, WASP immunoblot of Jurkat T cells stimulated with anti-CD3 mAb using mAb 5A5. **D**, Effect of pretreatment for 6 hours with calpeptin on anti-CD3–driven WASP degradation in peripheral blood T cells. Lysates were immunoblotted with mAb 5A5. *Nonspecific band. The positions of molecular weight markers are indicated on the *left* in Fig 1, *A* to *D*. The ratio of cleaved WASP to full-length *(FL)* WASP in Fig 1, *A* and *D*, represents the mean of 5 experiments. Similar results were obtained in Fig 1, *A* to *D*, in 5 independent experiments.

WASP fragment at 5 minutes, which increased at 10 and 15 minutes after stimulation. Scanning densitometric analysis revealed that the intensity of the cleaved WASP band was approximately 5% that of the full-length WASP band at 10 and 15 minutes after stimulation. Similar results were obtained in Jurkat T cells (Fig 1, *C*).

Immunoblotting lysates of T cells with the rabbit polyclonal antibody K374 raised against the C-terminal 20 amino acids of WASP revealed the same 62- to 64-kDa band detected by using mAb 5A5 but did not detect the 55-kDa WASP fragment in anti-CD3–stimulated T cells that was detected by using mAb 5A5 (Fig 1, *B*). Similar results were obtained in Jurkat T cells (data not shown). This result indicates that the 55-kDa WASP fragment lacks the C-terminal VCA domains of WASP (amino acids 421-502) responsible for its actin-polymerizing activity.

Calpain cleaves WASP *in vitro*[29] and contributes to WASP degradation in WIP-deficient T cells.[16,30] To examine whether calpain was responsible for the cleavage of WASP after TCR ligation, T cells were pretreated with the calpain inhibitor calpeptin for 6 hours, washed, and stimulated with anti-CD3 mAb for 5 minutes. Preincubation with calpeptin attenuated by approximately 50% the generation of the 55-kDa WASP fragment in response to anti-CD3 stimulation (Fig 1, *D*), strongly suggesting that calpain mediates the C-terminal truncation of WASP after TCR/CD3 ligation, at least in part.

WASP is ubiquitinated and degraded by the proteasome in T cells after TCR ligation

In the absence of WIP, WASP is degraded by the ubiquitin-proteasome pathway.[16,30] To investigate whether WASP is a substrate for ubiquitination, we incubated *in vitro* transcribed and translated WASP with purified ubiquitin and ubiquitin-conjugating enzymes (mixture of E1, E2, and E3 enzymes), and the reaction mixture was immunoblotted with anti-ubiquitin mAb. WASP was polyubiquitinated in the presence of ubiquitin and ubiquitin-conjugating enzymes, as indicated by an intense high-molecular-weight smear (Fig 2, *A*). Addition of the 26S proteasome fraction to the ubiquitination mixture resulted in marked attenuation of the ubiquitinated WASP smear. These results indicate that after TCR/CD3 ligation, WASP is subject to ubiquitination, which targets it for destruction by the proteasome.

We next examined whether WASP is ubiquitinated in T cells after TCR ligation. Fig 2, *B*, shows the appearance of polyubiquitinated WASP after anti-CD3 mAb stimulation of Jurkat T cells. To examine whether WASP ubiquitinated after TCR ligation is targeted for destruction by the proteasome, Jurkat T cells were pretreated with the proteasome inhibitor MG132 for 6 hours and then stimulated with anti-CD3 mAb for 10 minutes, and WASP immunoprecipitates were prepared from their lysates and probed for ubiquitin. Fig 2, *C*, shows that ubiquitinated WASP was weakly detectable in unstimulated Jurkat cells, but its levels increased after TCR/CD3 stimulation. Pretreatment with MG132 modestly increased the amounts of ubiquitinated WASP in unstimulated Jurkat cells and strongly increased the amounts of ubiquitinated WASP detected after TCR/CD3 ligation. These results indicate that WASP is ubiquitinated and degraded by the proteasome after TCR ligation.

The Cbl family proteins c-Cbl and Cbl-b associate with WASP after TCR ligation and act as E3 ubiquitin ligases for WASP

Members of the Cbl family of E3 ubiquitin ligases are negative regulators in TCR signaling.[31,32] We tested the hypothesis that Cbl proteins might be involved in WASP ubiquitination. We first

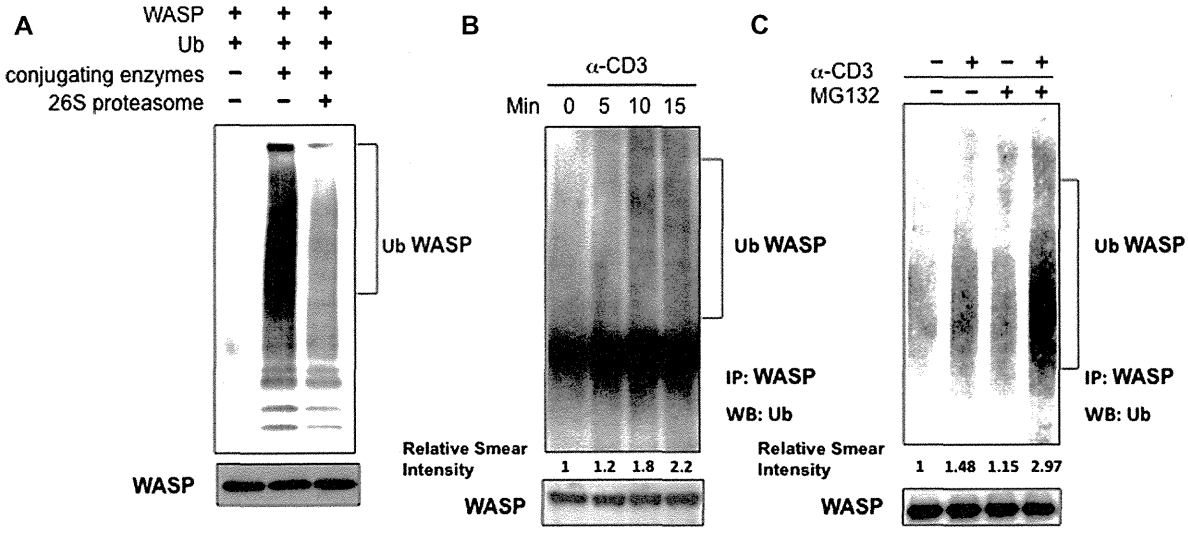

FIG 2. WASP is ubiquitinated and degraded by the 26S proteasome *in vitro* and in anti-CD3–stimulated Jurkat cells. **A,** Ubiquitination of *in vitro* translated purified WASP by ubiquitin-conjugating enzymes and its degradation by the 26S proteasome. Reaction mixtures were probed with anti-ubiquitin. **B,** Generation of ubiquitinated WASP in Jurkat T cells after stimulation with anti-CD3 mAb. WASP immunoprecipitates were probed with anti-ubiquitin mAb. Polyubiquitinated WASP appears as a smear. **C,** Protection of ubiquitinated WASP from degradation by the proteasome inhibitor MG132 in anti-CD3–stimulated Jurkat T cells. Similar results were obtained in Fig 2, *A* to *C*, in 4 independent experiments. The relative smear intensity in Fig 2, *B* and *C*, represents the mean of 4 experiments. *IP*, Immunoprecipitate; *Ub*, ubiquitin; *WB*, Western blot.

investigated whether Cbl proteins and WASP form a complex. WASP immunoprecipitates from Jurkat cell lysates were probed for c-Cbl and Cbl-b. c-Cbl, but not Cbl-b, coprecipitated weakly with WASP in unstimulated Jurkat T cells. TCR ligation increased the association of c-Cbl with WASP. It also induced the association of Cbl-b with WASP at 10 and 15 minutes after stimulation (Fig 3, *A*).

To investigate whether Cbl proteins act as E3 ubiquitin ligases for WASP, we transiently transfected 293T cells with plasmids coding for WT WASP, HA-tagged ubiquitin, FLAG-tagged c-Cbl, or FLAG-tagged Cbl-b. WASP coprecipitated with both c-Cbl and Cbl-b and was polyubiquitinated significantly more when co-transfected with ubiquitin, c-Cbl, and Cbl-b than with ubiquitin and empty vector (Fig 3, *B*).

To examine the role of Cbl-b in WASP ubiquitination after TCR ligation, we used purified T cells from spleens of *Cbl-b*$^{-/-}$ mice. Ubiquitination of WASP after TCR ligation was reduced, although not completely abrogated, in T cells from *Cbl-b*$^{-/-}$ mice (Fig 3, *C*), suggesting that WASP is a substrate for Cbl-b in antigen-stimulated T cells. We could not examine the role of c-Cbl on WASP ubiquitination after TCR ligation because we had no access to T cells from *c-Cbl*$^{-/-}$ mice.

WASP degradation after TCR/CD3 ligation limits TCR/CD3-driven F-actin assembly in T cells

WASP is important for F-actin assembly in T cells.[10] We examined whether WASP degradation after TCR/CD3 ligation regulates TCR/CD3-driven F-actin assembly. Purified T cells from WT and WASP-deficient mice were incubated for 6 hours with calpeptin or left untreated, washed and stimulated with anti-CD3 mAb, and cross-linked with a secondary antibody. The cells were then fixed, permeabilized, stained for F-actin with fluorescein isothiocyanate–conjugated phalloidin, and analyzed by means of flow cytometry. As previously reported, WASP-deficient T cells had a lower F-actin content than WT T cells.[16] TCR/CD3 ligation caused a parallel increase in F-actin levels in both WT and WASP-deficient T cells, which peaked at 5 minutes after stimulation and returned almost to baseline 10 minutes after stimulation. Pretreatment with calpeptin had no effect on F-actin content of the T cells at baseline or at 2 and 5 minutes after stimulation; however, it significantly increased the F-actin content of WT T cells at 10 minutes after anti-CD3 stimulation, maintaining it at almost the peak level achieved at 5 minutes after stimulation. In contrast, pretreatment with calpeptin had no effect on the F-actin content of WASP-deficient T cells 10 minutes after anti-CD3 stimulation. These results suggest that calpain-mediated WASP degradation limits the duration of F-actin assembly after TCR/CD3 ligation.

We next examined whether ubiquitination, which targets WASP for proteosomal degradation, regulates F-actin assembly after TCR/CD3 ligation. Because Cbl-b participates in WASP ubiquitination, we examined F-actin assembly in T cells deficient in Cbl-b. Baseline F-actin content and TCR-driven F-actin assembly were both significantly increased in T cells from c-Cbl-deficient mice compared with T cells from WT control animals (Fig 4, *B*). These results suggest that WASP degradation by ubiquitination regulates baseline and TCR-driven F-actin assembly.

DISCUSSION

Our results demonstrate that TCR ligation triggers the degradation of WASP by calpain-mediated cleavage and Cbl-mediated ubiquitination and subsequent proteasomal degradation. We present evidence that WASP degradation provides a mechanism for limiting the duration of TCR-driven assembly of F-actin.

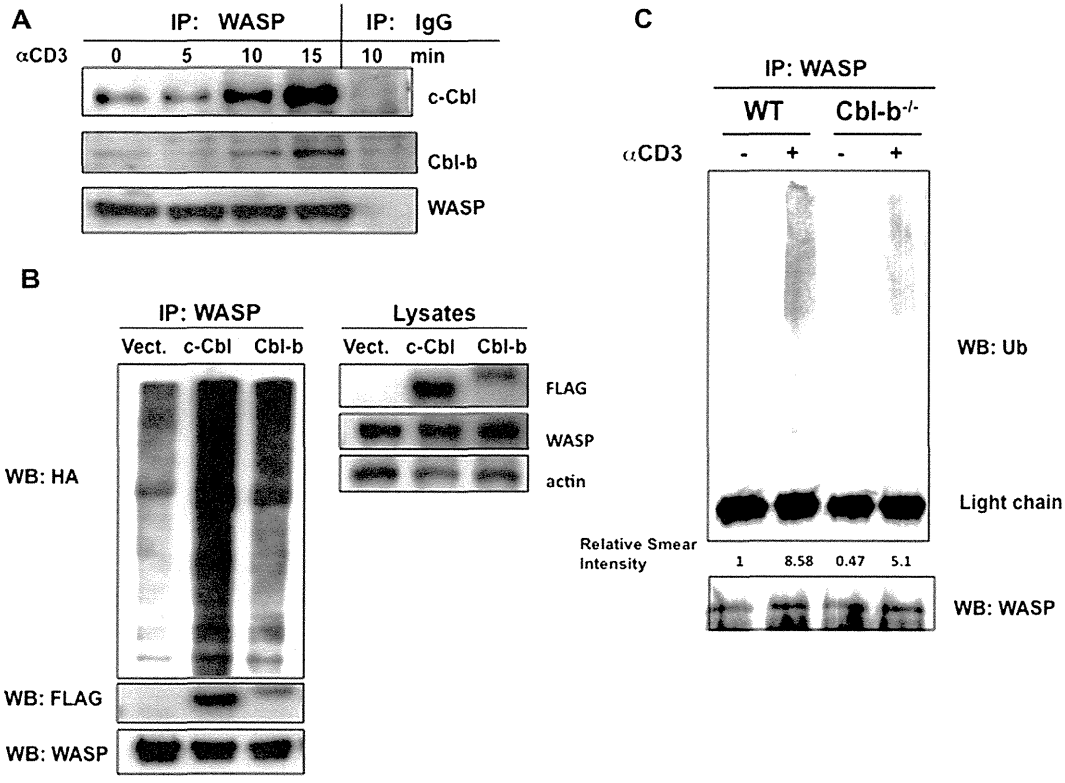

FIG 3. Cbl family E3 ubiquitin ligases associate with and ubiquitinate WASP after TCR ligation. **A,** Western blot analysis of WASP immunoprecipitates from anti-CD3–stimulated Jurkat T cells for c-Cbl and Cbl-b. IgG control antibody precipitates were prepared 10 minutes after anti-CD3 stimulation and used as controls. **B,** Ubiquitination of WASP in 293T cells transfected with WT WASP and HA-tagged ubiquitin plus either FLAG vector alone *(Vect.)*, FLAG-tagged c-Cbl, or FLAG-tagged Cbl-b. In the *left panel* WASP immunoprecipitates were probed for HA, FLAG, and WASP. In the *right panel* total lysates were probed for FLAG–c-Cbl or FLAG–Cbl-b, WASP, and actin. **C,** WASP ubiquitination after TCR ligation in T cells from *Cbl-b*$^{-/-}$ mice and WT control animals. WASP immunoprecipitates were probed for ubiquitin. Similar results were obtained in Fig 3, *A* to *C*, in 4 independent experiments. The relative smear intensity in Fig 3, *C*, represents the mean of 4 experiments. *IP*, Immunoprecipitate; *Ub*, ubiquitin; *WB*, Western blot.

TCR/CD3 ligation resulted in the degradation of a small fraction of WASP through calpain-mediated cleavage and the ubiquitin proteasome pathway. We estimated that approximately 5% of WASP is degraded after TCR/CD3 ligation. This is possibly an underestimate because the truncated 55-kDa WASP might be less stable than intact WASP. We could not detect a decrease in the levels of intact WASP in anti-CD3–activated T cells, probably because Western blotting is not sensitive enough to detect a small decrease in protein levels. We were unable to detect the cleaved, C-terminal, approximately 10-kDa fragment using an antibody to the C-terminus of WASP. This is most likely because such a small cleaved fragment would be rapidly degraded in the cell. Normally, WASP is protected from degradation by its partner, WIP.[16] The conformational changes in WASP induced by TCR signaling, which involve a change from an inactive to an active form capable of activating the Arp2/3 complex and F-actin polymerization, possibly increases the susceptibility of WASP to calpain cleavage and to ubiquitination and proteasomal degradation. The observation that WASP is degraded by calpain after TCR ligation is consistent with previous observations that WASP can be degraded in platelet lysates by calpain[29] and that *in vitro* translated WASP is a substrate for calpain I and II.[16] The increase in intracellular Ca^{++} concentration that follows TCR ligation could be the trigger for the Ca^{++}-dependent activation of calpain in anti-CD3–stimulated T cells.

Both c-Cbl and Cbl-b associated with WASP when overexpressed in 293T cells and acted as E3 ubiquitin ligases for WASP ubiquitination *in vitro*. More importantly, WASP ubiquitination after TCR ligation was impaired in Cbl-b-deficient T cells, implicating at least Cbl-b in WASP ubiquitination in T cells. Cbl family proteins act as negative regulators of TCR signaling by virtue of their ability to ubiquitinate LCK and ZAP-70,[33] which are upstream of WASP. Thus Cbl family members might regulate WASP activity indirectly by dampening TCR signaling upstream of WASP, as well as directly by ubiquitinating WASP and targeting it for degradation. Evidence has been presented that the activated WASP phosphorylated at Y291 is a target for ubiquitination.[34] We have also found that inhibition of the proteasome by MG132 increases the amount of tyrosine-phosphorylated WASP in anti-CD3–stimulated cells (see Fig E1 in this article's Online Repository at www.jacionline.org). This observation lends further support to the notion that activated WASP molecules are targets for degradation after TCR ligation.

It is not clear whether the interaction between WASP and c-Cbl and Cbl-b is direct or mediated by other proteins. It has been reported that c-Cbl associates with multiple proteins, which

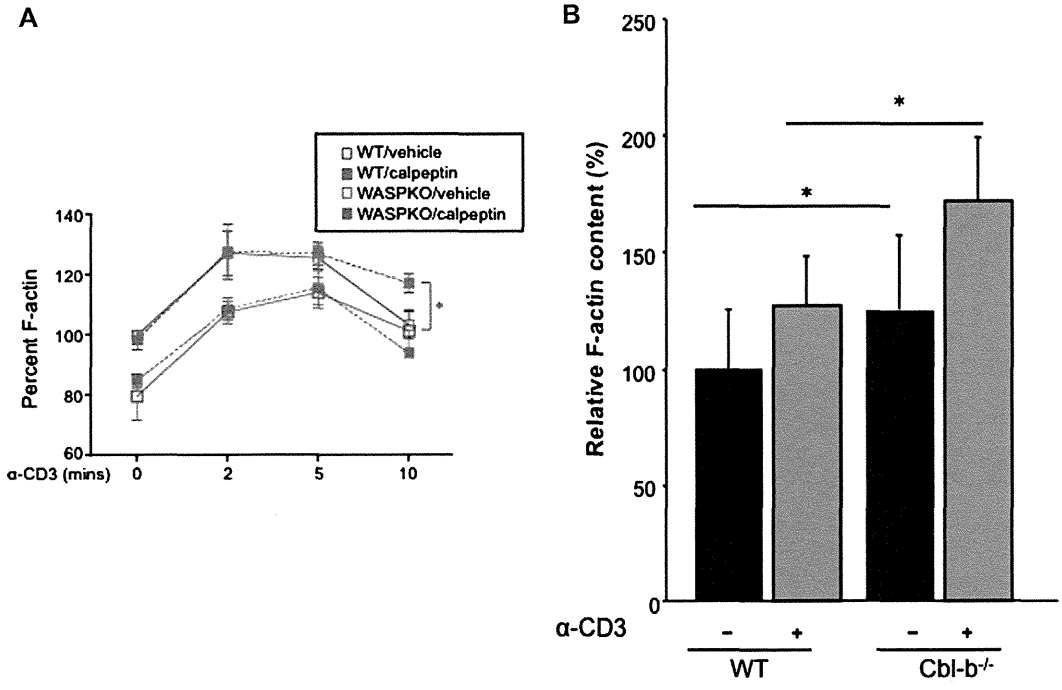

FIG 4. Effect of calpain inhibition and loss of Cbl on F-actin assembly in T cells. **A,** Effect of pretreatment of T cells from WT and WASP knockout mice with calpeptin on TCR-driven assembly of F-actin. Pretreatment with the vehicle dimethyl sulfoxide was used as a control. **B,** TCR-driven assembly of F-actin in T cells from *Cbl-b*$^{-/-}$ mice and WT control animals. T cells were stimulated with anti-CD3 for 10 minutes. Results are expressed as a percentage of the baseline F-actin content in unstimulated WT T cells and represent the means ± SDs of 3 independent experiments. **P* < .01.

include tyrosine phosphorylated ZAP-70,[35] the adaptor proteins Nck[36] and Grb2[37] through their SH3 domains, CrkL through its SH2 domain,[38] Src tyrosine kinases through their SH3 domains,[39,40] and Vav and the p85 regulatory subunit of phosphatidylinositol-3-OH kinase through their SH2 domains.[41,42] Because these proteins are also reported to associate with WASP, its partner WIP, or both,[17,43] an indirect association of Cbl with WASP cannot be ruled out. Alternatively, c-Cbl and Cbl-b could directly interact with an activated form of WASP, such as tyrosine-phosphorylated WASP. Indeed, while this manuscript was in preparation, it was shown that WASP phosphorylation at tyrosine 291 after TCR activation results in recruitment of Cbl-b.[34]

Our data suggest that the degraded fraction of WASP includes activated WASP. This is supported by the observation that calpain inhibition and lack of the WASP-ubiquitinating E3 ligase Cbl-b resulted in more sustained F-actin assembly in WT T cells after TCR/CD3 ligation. The small fraction of WASP that is cleaved after TCR ligation could be important for F-actin polymerization because of its location close to the TCR. Indeed, we have shown previously that a fraction of WASP translocates together with a fraction of the TCR/CD3 complex to lipid rafts.[17] It is also well known that a fraction of WASP colocalizes with TCR molecules in the immune synapse (IS).[17,44,45] Cbl family molecules, which are also recruited to the IS, where they are activated by LCK and ZAP-70,[46,47] could ubiquitinate WASP molecules recruited to the IS, targeting them for degradation. The IS is a dynamic structure that constantly undergoes protein kinase Cθ–dependent dissolution and WASP/F-actin–dependent reformation of its peripheral supramolecular activation complex.[45] Protein kinase Cθ–dependent dissolution breaks the symmetry of the IS and allows T-cell motility. WASP/F-actin–dependent reformation of the IS is important for the sustained signaling that is necessary for IL-2 production. We speculate that cycles of TCR-triggered recruitment and activation of WASP in the IS followed by local degradation of the activated WASP might be important for IS dynamics and T-cell function.

The observation that baseline F-actin content was increased in *Cbl-b*$^{-/-}$ T cells, but not in calpeptin-treated T cells, suggests that under steady-state conditions, Cbl ubiquitination and proteasome degradation, but not calpain, degrade WASP molecules in activated in T cells. The observation that calpain inhibition had no effect on F-actin assembly in WASP-deficient T cells indicates that calpain regulates F-actin assembly by targeting WASP for degradation. These results strongly suggest that degradation of activated WASP by calpain and by the ubiquitin/proteasome pathway provide an important homeostatic mechanism for terminating signaling to the cytoskeleton after TCR ligation. Furthermore, WASP mutants that are resistant to ubiquitination are associated with enhanced T-cell activation, supporting the notion that WASP degradation limits TCR activation.[34]

Protein cleavage is used by prokaryotes and eukaryotes to activate or terminate signaling. Well-documented examples include the coagulation cascade, the complement activation cascade, degradation of the nuclear factor κB inhibitor IκBα, TNF receptor–associated factor 3, Argonaute, and voltage-gated calcium-channel proteins.[48-53] Degradation of activated WASP might regulate receptor signaling to the cytoskeleton not only in T cells but also in other hematopoietic cells. Such a control mechanism would avoid the potential pathology observed in patients with mutations that cause sustained WASP activation and manifest as X-linked neutropenia.

We thank K. A. Siminovitch, H. Gu, N. Ishii, and Y. Tanaka for reagents and mice.

Key message

- **TCR signaling causes WASP to be degraded by calpain and by Cbl-family members through ubiquitination and destruction by the proteasome, limiting TCR-driven assembly of F-actin.**

REFERENCES

1. Ochs HD, Rosen FS. The Wiskott-Aldrich syndrome. 2nd ed. New York: Oxford University Press; 2006.
2. Derry JMJ, Ochs HD, Francke U. Isolation of a novel gene mutated in Wiskott-Aldrich syndrome. Cell 1994;78:635-44.
3. Kwan SP, Hagemann TL, Radtke BE, Blaese RM, Rosen FS. Identification of mutations in the Wiskott-Aldrich syndrome gene and characterization of a polymorphic dinucleotide repeat at DXS6940, adjacent to the disease gene. Proc Natl Acad Sci U S A 1995;92:4706-10.
4. Anton IM, Jones GE, Wandosell F, Geha R, Ramesh N. WASP-interacting protein (WIP): working in polymerisation and much more. Trends Cell Biol 2007;17:555-62.
5. Higgs HN, Pollard TD. Activation by Cdc42 and PIP2 of Wiskott-Aldrich syndrome protein (WASp) stimulates actin nucleation by Arp2/3 complex. J Cell Biol 2000;150:1311-20.
6. Ramesh N, Anton IM, Hartwig JH, Geha RS. WIP, a protein associated with Wiskott-Aldrich syndrome protein, induces actin polymerization and redistribution in lymphoid cells. Proc Natl Acad Sci U S A 1997;94:14671-6.
7. Badour K, Zhang J, Siminovitch KA. Involvement of the Wiskott-Aldrich syndrome protein and other actin regulatory adaptors in T cell activation. Semin Immunol 2004;16:395-407.
8. Huang Y, Burkhardt JK. T-cell-receptor-dependent actin regulatory mechanisms. J Cell Sci 2007;120:723-30.
9. Thrasher AJ. WASp in immune-system organization and function. Nat Rev Immunol 2002;2:635-46.
10. Gallego MD, Santamaria M, Pena J, Molina IJ. Defective actin reorganization and polymerization of Wiskott-Aldrich T cells in response to CD3-mediated stimulation. Blood 1997;90:3089-97.
11. Snapper SB, Rosen FS, Mizoguchi E, Cohen P, Khan W, Liu C-H, et al. Wiskott-Aldrich Syndrome protein-deficient mice reveal a role for WASP in T but not B cell activation. Immunity 1998;9:81-91.
12. Zhang J, Shehabeldin A, da Cruz LA, Butler J, Somani AK, McGavin M, et al. Antigen receptor-induced activation and cytoskeletal rearrangement are impaired in Wiskott-Aldrich syndrome protein-deficient lymphocytes. J Exp Med 1999;190:1329-42.
13. Cory GO, Garg R, Cramer R, Ridley AJ. Phosphorylation of tyrosine 291 enhances the ability of WASp to stimulate actin polymerization and filopodium formation. J Biol Chem 2002;277:45115-21.
14. Rohatgi R, Nollau P, Ho HY, Kirschner MW, Mayer BJ. Nck and phosphatidylinositol 4,5-bisphosphate synergistically activate actin polymerization through the N-WASP-Arp2/3 pathway. J Biol Chem 2001;276:26448-52.
15. Torres E, Rosen MK. Contingent phosphorylation/dephosphorylation provides a mechanism of molecular memory in WASP. Mol Cell 2003;11:1215-27.
16. de la Fuente MA, Sasahara Y, Calamito M, Anton IM, Elkhal A, Gallego MD, et al. WIP is a chaperone for Wiskott-Aldrich syndrome protein (WASP). Proc Natl Acad Sci U S A 2007;104:926-31.
17. Sasahara Y, Rachid R, Byrne MJ, de la Fuente MA, Abraham RT, Ramesh N, et al. Mechanism of recruitment of WASP to the immunological synapse and of its activation following TCR ligation. Mol Cell 2002;10:1269-81.
18. Lanzi G, Moratto D, Vairo D, Masneri S, Delmonte O, Paganini T, et al. A novel primary human immunodeficiency due to deficiency in the WASP-interacting protein WIP. J Exp Med 2012;209:29-34.
19. Moratto D, Giliani S, Notarangelo LD, Mazza C, Mazzolari E, Notarangelo LD. The Wiskott-Aldrich syndrome: from genotype-phenotype correlation to treatment. Expert Rev Clin Immunol 2007;3:813-24.
20. Ochs HD, Notarangelo LD. Structure and function of the Wiskott-Aldrich syndrome protein. Curr Opin Hematol 2005;12:284-91.
21. Massaad MJ, Ramesh N, Le Bras S, Giliani S, Notarangelo LD, Al-Herz W, et al. A peptide derived from the Wiskott-Aldrich syndrome (WAS) protein-interacting protein (WIP) restores WAS protein level and actin cytoskeleton reorganization in lymphocytes from patients with WAS mutations that disrupt WIP binding. J Allergy Clin Immunol 2011;127:998-1005, e1-2.
22. Devriendt K, Kim AS, Mathijs G, Frints SG, Schwartz M, Van Den Oord JJ, et al. Constitutively activating mutation in WASP causes X-linked severe congenital neutropenia. Nat Genet 2001;27:313-7.
23. Ochs HD. Mutations of the Wiskott-Aldrich syndrome protein affect protein expression and dictate the clinical phenotypes. Immunol Res 2009;44:84-8.
24. Beel K, Cotter MM, Blatny J, Bond J, Lucas G, Green F, et al. A large kindred with X-linked neutropenia with an I294T mutation of the Wiskott-Aldrich syndrome gene. Br J Haematol 2009;144:120-6.
25. Westerberg LS, Meelu P, Baptista M, Eston MA, Adamovich DA, Cotta-de-Almeida V, et al. Activating WASP mutations associated with X-linked neutropenia result in enhanced actin polymerization, altered cytoskeletal responses, and genomic instability in lymphocytes. J Exp Med 2010;207:1145-52.
26. Kawai S, Minegishi M, Ohashi Y, Sasahara Y, Kumaki S, Konno T, et al. Flow cytometric determination of intracytoplasmic Wiskott-Aldrich syndrome protein in peripheral blood lymphocyte subpopulations. J Immunol Methods 2002;260:195-205.
27. Tanaka Y, Tanaka N, Saeki Y, Tanaka K, Murakami M, Hirano T, et al. c-Cbl-dependent monoubiquitination and lysosomal degradation of gp130. Mol Cell Biol 2008;28:4805-18.
28. Du W, Kumaki S, Uchiyama T, Yachie A, Yeng Looi C, Kawai S, et al. A second-site mutation in the initiation codon of WAS (WASP) results in expansion of subsets of lymphocytes in an Wiskott-Aldrich syndrome patient. Hum Mutat 2006; 27:370-5.
29. Shcherbina A, Miki H, Kenney DM, Rosen FS, Remold-O'Donnell E. WASP and N-WASP in human platelets differ in sensitivity to protease calpain. Blood 2001; 98:2988-91.
30. Chou HC, Anton IM, Holt MR, Curcio C, Lanzardo S, Worth A, et al. WIP regulates the stability and localization of WASP to podosomes in migrating dendritic cells. Curr Biol 2006;16:2337-44.
31. Bachmaier K, Krawczyk C, Kozieradzki I, Kong YY, Sasaki T, Oliveira-dos-Santos A, et al. Negative regulation of lymphocyte activation and autoimmunity by the molecular adaptor Cbl-b. Nature 2000;403:211-6.
32. Paolino M, Penninger JM. Cbl-b in T-cell activation. Semin Immunopathol 2010; 32:137-48.
33. Krawczyk C, Penninger JM. Molecular controls of antigen receptor clustering and autoimmunity. Trends Cell Biol 2001;11:212-20.
34. Reicher B, Joseph N, David A, Pauker MH, Perl O, Barda-Saad M. Ubiquitylation-dependent negative regulation of WASp is essential for actin cytoskeleton dynamics. Mol Cell Biol 2012;32:3153-63.
35. Lupher ML Jr, Reedquist KA, Miyake S, Langdon WY, Band H. A novel phosphotyrosine-binding domain in the N-terminal transforming region of Cbl interacts directly and selectively with ZAP-70 in T cells. J Biol Chem 1996;271: 24063-8.
36. Miyoshi-Akiyama T, Aleman LM, Smith JM, Adler CE, Mayer BJ. Regulation of Cbl phosphorylation by the Abl tyrosine kinase and the Nck SH2/SH3 adaptor. Oncogene 2001;20:4058-69.
37. Donovan JA, Ota Y, Langdon WY, Samelson LE. Regulation of the association of p120cbl with Grb2 in Jurkat T cells. J Biol Chem 1996;271:26369-74.
38. Gesbert F, Garbay C, Bertoglio J. Interleukin-2 stimulation induces tyrosine phosphorylation of p120-Cbl and CrkL and formation of multimolecular signaling complexes in T lymphocytes and natural killer cells. J Biol Chem 1998;273: 3986-93.
39. Reedquist KA, Fukazawa T, Panchamoorthy G, Langdon WY, Shoelson SE, Druker BJ, et al. Stimulation through the T cell receptor induces Cbl association with Crk proteins and the guanine nucleotide exchange protein C3G. J Biol Chem 1996;271:8435-42.
40. Tanaka S, Neff L, Baron R, Levy JB. Tyrosine phosphorylation and translocation of the c-cbl protein after activation of tyrosine kinase signaling pathways. J Biol Chem 1995;270:14347-51.
41. Jain SK, Langdon WY, Varticovski L. Tyrosine phosphorylation of p120cbl in BCR/abl transformed hematopoietic cells mediates enhanced association with phosphatidylinositol 3-kinase. Oncogene 1997;14:2217-28.
42. Tartare-Deckert S, Monthouel MN, Charvet C, Foucault I, Van Obberghen E, Bernard A, et al. Vav2 activates c-fos serum response element and CD69 expression but negatively regulates nuclear factor of activated T cells and interleukin-2 gene activation in T lymphocyte. J Biol Chem 2001;276:20849-57.
43. Anton IM, Lu W, Mayer BJ, Ramesh N, Geha RS. The Wiskott-Aldrich syndrome protein-interacting protein (WIP) binds to the adaptor protein Nck. J Biol Chem 1998;273:20992-5.
44. Cannon JL, Labno CM, Bosco G, Seth A, McGavin MH, Siminovitch KA, et al. Wasp recruitment to the T cell:APC contact site occurs independently of Cdc42 activation. Immunity 2001;15:249-59.
45. Sims TN, Soos TJ, Xenias HS, Dubin-Thaler B, Hofman JM, Waite JC, et al. Opposing effects of PKCtheta and WASp on symmetry breaking and relocation of the immunological synapse. Cell 2007;129:773-85.

46. Elly C, Witte S, Zhang Z, Rosnet O, Lipkowitz S, Altman A, et al. Tyrosine phosphorylation and complex formation of Cbl-b upon T cell receptor stimulation. Oncogene 1999;18:1147-56.
47. Wiedemann A, Muller S, Favier B, Penna D, Guiraud M, Delmas C, et al. T-cell activation is accompanied by an ubiquitination process occurring at the immunological synapse. Immunol Lett 2005;98:57-61.
48. Schenone M, Furie BC, Furie B. The blood coagulation cascade. Curr Opin Hematol 2004;11:272-7.
49. Forneris F, Wu J, Gros P. The modular serine proteases of the complement cascade. Curr Opin Struct Biol 2012;22:333-41.
50. Baud V, Derudder E. Control of NF-kappaB activity by proteolysis. Curr Top Microbiol Immunol 2011;349:97-114.
51. Bronevetsky Y, Villarino AV, Eisley CJ, Barbeau R, Barczak AJ, Heinz GA, et al. T cell activation induces proteasomal degradation of Argonaute and rapid remodeling of the microRNA repertoire. J Exp Med 2013;210:417-32.
52. Razani B, Reichardt AD, Cheng G. Non-canonical NF-kappaB signaling activation and regulation: principles and perspectives. Immunol Rev 2011;244:44-54.
53. De Jongh KS, Colvin AA, Wang KK, Catterall WA. Differential proteolysis of the full-length form of the L-type calcium channel alpha 1 subunit by calpain. J Neurochem 1994;63:1558-64.

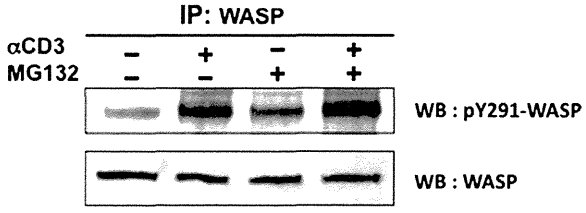

FIG E1. Tyrosine-phosphorylated WASP generated after TCR ligation is a target for proteasomal degradation. Effect of pretreatment of MG132 on the amount of tyrosine-phosphorylated WASP in anti-CD3–stimulated Jurkat T cells is shown. WASP immunoprecipitates were probed with anti-pY291-WASP antibody (Abcam). Similar results were obtained in 3 experiments. *IP*, Immunoprecipitate; *WB*, Western blot.

nature genetics

Variants in *CPA1* are strongly associated with early onset chronic pancreatitis

Heiko Witt[1–3], Sebastian Beer[4,44], Jonas Rosendahl[5,44], Jian-Min Chen[6,7,44], Giriraj Ratan Chandak[8,44], Atsushi Masamune[9,44], Melinda Bence[4,44], Richárd Szmola[4,10,44], Grzegorz Oracz[11], Milan Macek Jr[12], Eesh Bhatia[13], Sandra Steigenberger[1,2], Denise Lasher[1,2], Florence Bühler[1,2], Catherine Delaporte[1,2], Johanna Tebbing[1,2], Maren Ludwig[1,2], Claudia Pilsak[1,2], Karolin Saum[1,2], Peter Bugert[14], Emmanuelle Masson[6,7], Sumit Paliwal[8], Seema Bhaskar[8], Agnieszka Sobczynska-Tomaszewska[15,16], Daniel Bak[16], Ivan Balascak[17], Gourdas Choudhuri[18], D Nageshwar Reddy[19], G Venkat Rao[19], Varghese Thomas[20], Kiyoshi Kume[9], Eriko Nakano[9], Yoichi Kakuta[9], Tooru Shimosegawa[9], Lukasz Durko[21], András Szabó[4], Andrea Schnúr[4,22], Péter Hegyi[22], Zoltán Rakonczay Jr[22], Roland Pfützer[23], Alexander Schneider[24], David Alexander Groneberg[25], Markus Braun[25], Hartmut Schmidt[26], Ulrike Witt[27], Helmut Friess[27], Hana Algül[28], Olfert Landt[29], Markus Schuelke[30,31], Renate Krüger[32], Bertram Wiedenmann[33], Frank Schmidt[34], Klaus-Peter Zimmer[35], Peter Kovacs[36,37], Michael Stumvoll[36,37], Matthias Blüher[36,37], Thomas Müller[38], Andreas Janecke[38,39], Niels Teich[40], Robert Grützmann[41], Hans-Ulrich Schulz[42], Joachim Mössner[5], Volker Keim[5], Matthias Löhr[43], Claude Férec[6,7] & Miklós Sahin-Tóth[4]

Chronic pancreatitis is an inflammatory disorder of the pancreas. We analyzed *CPA1*, encoding carboxypeptidase A1, in subjects with nonalcoholic chronic pancreatitis (cases) and controls in a German discovery set and three replication sets. Functionally impaired variants were present in 29/944 (3.1%) German cases and 5/3,938 (0.1%) controls (odds ratio (OR) = 24.9, $P = 1.5 \times 10^{-16}$). The association was strongest in subjects aged ≤10 years (9.7%; OR = 84.0, $P = 4.1 \times 10^{-24}$). In the replication sets, defective *CPA1* variants were present in 8/600 (1.3%) cases and 9/2,432 (0.4%) controls from Europe ($P = 0.01$), 5/230 (2.2%) cases and 0/264 controls from India ($P = 0.02$) and 5/247 (2.0%) cases and 0/341 controls from Japan ($P = 0.013$). The mechanism by which *CPA1* variants confer increased pancreatitis risk may involve misfolding-induced endoplasmic reticulum stress rather than elevated trypsin activity, as is seen with other genetic risk factors for this disease.

Chronic pancreatitis is an inflammatory condition that is characterized by abdominal pain and progressive damage to both exocrine and endocrine components of the pancreas, resulting in insufficiency of the organ with maldigestion and diabetes. Although alcohol abuse has long been recognized as a major risk factor for chronic pancreatitis, genetic susceptibility has emerged during the last two decades as a strong determinant of disease risk, particularly in the pediatric population[1].

Genetic studies performed so far have suggested that the development of intrapancreatic trypsin activity has a central role in disease pathogenesis. Thus, gain-of-function mutations in the gene encoding cationic trypsinogen (*PRSS1*, MIM276000) as well as loss-of-function variants in the genes encoding the pancreatic secretory trypsin inhibitor (*SPINK1*, MIM167790) and the trypsinogen-degrading enzyme chymotrypsin C (*CTRC*, MIM601405) increase the risk for chronic pancreatitis[2–8]. Consistent with the proposed pathogenic role of trypsin, a rapidly autodegrading variant of the gene encoding anionic trypsinogen (*PRSS2*, MIM601564) and a common *PRSS1* promoter variant protect against chronic pancreatitis[9,10].

Despite these recent advances, we still find that many individuals with chronic pancreatitis do not carry mutations in any of the known susceptibility genes, suggesting the involvement of other yet unidentified genes. In the present study, we investigated the role of *CPA1* in individuals with chronic pancreatitis. Digestive carboxypeptidases are pancreatic metalloproteases that hydrolyze C-terminal peptide bonds in dietary polypeptide chains[11]. Three different isoforms have been described in human pancreatic juice. A-type carboxypeptidases (CPA1 and CPA2) act on aromatic and aliphatic amino acid residues that are exposed by the action of chymotrypsins and elastases, whereas the B-type carboxypeptidase (CPB1) hydrolyzes C-terminal lysine and arginine residues generated by tryptic cleavages[11]. The gene encoding human CPA1 (MIM114850) maps to 7q32.2, spans approximately 8 kb and contains 10 exons. The inactive preproprotein comprises 419 amino acids, including a

A full list of author affiliations appears at the end of the paper.

Received 18 April; accepted 23 July; published online 18 August 2013; doi:10.1038/ng.2730

Table 1 Nonsynonymous *CPA1* variants in German subjects with nonalcoholic chronic pancreatitis and healthy controls

Exon	Nucleotide change	Amino acid change	Cases (%) (n = 944)	Controls (%) (n = 3,938)	P	OR	95% CI	Apparent activity	Secretion level
1	c.5G>A	p.Arg2Gln	0 (0)	2 (0.05)	1.0	–	–	103	92
2	**c.79C>T**	**p.Arg27Ter**	**0 (0)**	**2 (0.05)**	**1.0**	**–**	**–**	**0**	**0**
2	c.101C>T	p.Ala34Val	0 (0)	1 (0.03)	1.0	–	–	98	97
3	c.197G>A	p.Arg66Gln	0 (0)	2 (0.05)	1.0	–	–	60	55
3	c.281A>G	p.Gln94Arg	1 (0.1)	13 (0.3)	0.5	–	–	57	57
3	c.321C>G	p.Phe107Leu	0 (0)	1 (0.03)	1.0	–	–	112	100
3	c.371C>T	p.Thr124Ile	8 (0.9)	45 (1.1)	0.6	–	–	23	27
4	c.410C>G	p.Ala137Gly	1 (0.1)	0 (0)	0.2	–	–	52	56
5	c.497G>A	p.Gly166Asp	5 (0.5)	20 (0.5)	1.0	–	–	73	66
5	**c.542G>A**	**p.Arg181Gln**	**0 (0)**	**1 (0.03)**	**1.0**	**–**	**–**	**1**	**39**
6	c.622G>A	p.Ala208Thr (het)	71 (7.5)	266 (6.8)	0.4	–	–	81	73
6	c.622G>A	p.Ala208Thr (hom)	1 (0.1)	1 (0.03)	0.4	–	–	–	–
6	c.622G>T	p.Ala208Ser	0 (0)	1 (0.03)	1.0	–	–	91	83
6	**c.673G>A**	**p.Gly225Ser**	**1 (0.1)**	**0 (0)**	**0.2**	**–**	**–**	**4**	**12**
7	**c.710G>A**	**p.Arg237His**	**0 (0)**	**2 (0.05)**	**1.0**	**–**	**–**	**0**	**81**
7	**c.751G>A**	**p.Val251Met**	**2 (0.2)**	**0 (0)**	**0.1**	**–**	**–**	**0**	**0**
7	**c.758C>G**	**p.Pro253Arg**	**1 (0.1)**	**0 (0)**	**0.2**	**–**	**–**	**0**	**0**
7	**c.768C>G**	**p.Asn256Lys**	**7 (0.7)**	**0 (0)**	**9.9×10^{-6}**	**NC**	**NC**	**0**	**0**
7	c.775G>A	p.Ala259Thr	0 (0)	1 (0.03)	1.0	–	–	85	82
8	**c.811T>C**	**p.Cys271Arg**	**1 (0.1)**	**0 (0)**	**0.2**	**–**	**–**	**1**	**0**
8	**c.829G>A**	**p.Gly277Ser**	**1 (0.1)**	**0 (0)**	**0.2**	**–**	**–**	**0**	**0**
8	**c.839C>A**	**p.Ala280Asp**	**1 (0.1)**	**0 (0)**	**0.2**	**–**	**–**	**0**	**5**
8	**c.847G>A**	**p.Glu283Lys**	**2 (0.2)**	**0 (0)**	**0.1**	**–**	**–**	**0**	**0**
8	**c.982G>A**	**p.Glu328Lys**	**1 (0.1)**	**0 (0)**	**0.2**	**–**	**–**	**9**	**42**
9	c.1009G>C	p.Val337Leu	0 (0)	1 (0.03)	1.0	–	–	64	61
Intron 9	**c.1073-2A>G**	**p.Tyr358fs[a]**	**3 (0.3)**	**0 (0)**	**0.007**	**NC**	**NC**	**0**	**0**
10	**c.1085G>A**	**p.Gly362Glu**	**1 (0.1)**	**0 (0)**	**0.2**	**–**	**–**	**0**	**6**
10	**c.1126T>C**	**p.Ser376Pro**	**2 (0.2)**	**0 (0)**	**0.1**	**–**	**–**	**0**	**7**
10	**c.1144C>T**	**p.Arg382Trp**	**5 (0.5)**	**0 (0)**	**0.0003**	**NC**	**NC**	**0**	**31**
10	c.1157G>A	p.Arg386His	0 (0)	1 (0.03)	1.0	–	–	92	97
10	c.1193C>T	p.Pro398Leu	0 (0)	1 (0.03)	1.0	–	–	42	64
10	c.1217C>G	p.Ala406Gly	0 (0)	1 (0.03)	1.0	–	–	137	114
10	**c.1247delA**	**p.Asn416fs**	**1 (0.1)**	**0 (0)**	**0.2**	**–**	**–**	**11**	**15**
10	c.1251C>A	p.His417Gln	0 (0)	1 (0.03)	1.0	–	–	62	54
10	c.1253C>T	p.Pro418Leu	0 (0)	1 (0.03)	1.0	–	–	91	99
All variants with apparent activity <20%			**29 (3.1%)**	**5 (0.1)**	**1.5×10^{-16}**	**24.9**	**9.6–64.6**	**–**	**–**

P values were determined by Fisher's exact test. Apparent CPA1 activity and secretion levels are expressed as a percentage of the wild-type values. Apparent activity corresponds to the CPA1 activity measured in the conditioned medium of transfected cells after activation with trypsin and CTRC (Online Methods). Thus, the apparent activity reflects the combined effects of the variants on secretion, catalytic activity and degradation by trypsin and/or CTRC. Secretion level indicates the concentration of proCPA1 in the conditioned medium measured by SDS-PAGE and densitometry (Online Methods). Alterations in bold indicate variants with less than 20% apparent activity.

[a]A splice-site variant that was modeled functionally as intron retention (as described in the **Supplementary Note**). Het, heterozygous; hom, homozygous; NC, not calculated, as the variant was not detected in the controls, rendering the OR infinite.

16-amino-acid secretory signal peptide and a 94-amino-acid propeptide. Activation of the proenzyme (proCPA1) to CPA1 is catalyzed by the sequential action of trypsin and CTRC, which cleave and degrade the propeptide[12]. After trypsinogens, proCPA1 is the second largest component of pancreatic juice, contributing more than 10% of the total protein[13].

We performed direct DNA sequencing of all ten *CPA1* exons in 944 cases and 3,938 control subjects of German origin. Considering variants in the coding regions and flanking splice sites, we identified 31 missense variants, 1 nonsense variant, 1 frame-shift variant and 1 splice-site variant and found that 3 variants were significantly enriched in cases (**Table 1**). Functional analysis demonstrated that 17/34 (50%) variants resulted in a marked (>80%) loss of apparent CPA1 activity, a term we use to describe the combined effects of the variants on secretion, proteolytic stability and catalytic competence (**Table 1**, **Supplementary Fig. 1** and Online Methods). The majority of these variants were located in exons 7, 8 and 10. Notably, 14 out of 17 (82%) functionally impaired variants were present in cases exclusively, including the c.768C>G (p.Asn256Lys) variant, which we detected in seven cases. Thus, *CPA1* variants with less than 20% apparent activity were significantly over-represented in the chronic pancreatitis group (29/944, 3.1%) as compared to in controls (5/3,938, 0.1%) (OR = 24.9, 95% confidence interval (CI) 9.6–64.6, $P = 1.5 \times 10^{-16}$) (**Table 1**). No individual was compound heterozygous or

Table 2 Distribution of functionally impaired *CPA1* variants in different age groups of German subjects with nonalcoholic chronic pancreatitis

Age of cases	Cases (%)	Controls (%)	P	OR	95% CI
All	29/944 (3.1)	5/3,938 (0.1)	1.5×10^{-16}	24.9	9.6–64.6
>20 years	2/358 (0.6)	5/3,938 (0.1)	0.2	–	–
≤20 years	27/586 (4.6)	5/3,938 (0.1)	6.8×10^{-20}	38.0	14.6–99.1
≤10 years	22/228 (9.7)	5/3,938 (0.1)	4.1×10^{-24}	84.0	31.5–224.1

P values were determined by Fisher's exact test. Alterations with less than 20% apparent activity were included.

Table 3 Nonsynonymous *CPA1* variants in the European replication study

Exon	Nucleotide change	Amino acid change	Cases (%) (n = 600)	Controls (%) (n = 2,432)	P	OR	95% CI	Apparent activity	Secretion level
1	c.5G>A	p.Arg2Gln	0 (0)	6 (0.2)	0.6	–	–	103	92
2	**c.79C>T**	**p.Arg27Ter**	**1 (0.2)**	**5 (0.2)**	**0.7**	**–**	**–**	**0**	**0**
2	**c.80G>C**	**p.Arg27Pro**	**0 (0)**	**1 (0.04)**	**1.0**	**–**	**–**	**0**	**0**
Intron 2	**c.148-1G>A**	**p.Leu50_Glu127del[a]**	**0 (0)**	**1 (0.04)**	**1.0**	**–**	**–**	**0**	**0**
3	c.197G>A	p.Arg66Gln	0 (0)	1 (0.04)	1.0	–	–	60	55
3	c.241T>C	p.Ser81Pro	0 (0)	1 (0.04)	1.0	–	–	53	57
3	c.281A>G	p.Gln94Arg	0 (0)	9 (0.4)	1.0	–	–	57	57
3	c.313T>C	p.Phe105Leu	1 (0.2)	0 (0)	0.2	–	–	109	99
3	c.334C>T	p.Arg112Cys	1 (0.2)	0 (0)	0.2	–	–	69	78
3	c.371C>T	p.Thr124Ile	3 (0.5)	14 (0.6)	1.0	–	–	23	27
4	c.389A>C	p.Asp130Ala	0 (0)	1 (0.04)	1.0	–	–	77	68
5	c.497G>A	p.Gly166Asp	1 (0.2)	11 (0.5)	0.5	–	–	73	66
6	c.604C>A	p.Gln202Lys	1 (0.2)	0 (0)	0.2	–	–	114	104
6	c.622G>A	p.Ala208Thr	45 (7.5)[b]	143 (5.9)[b]	0.1	–	–	81	73
6	**c.686C>T**	**p.Thr229Met**	**0 (0)**	**1 (0.04)**	**1.0**	**–**	**–**	**0**	**0**
6	c.695C>T	p.Thr232Met	1 (0.2)	0 (0)	0.2	–	–	87	80
7	**c.751G>A**	**p.Val251Met**	**1 (0.2)**	**0 (0)**	**0.2**	**–**	**–**	**0**	**0**
8	**c.809C>G**	**p.Pro270Arg**	**1 (0.2)**	**0 (0)**	**0.2**	**–**	**–**	**9**	**14**
8	**c.941A>G**	**p.Tyr314Cys**	**1 (0.2)**	**0 (0)**	**0.2**	**–**	**–**	**0**	**23**
8	**c.954_955delCA**	**p.Tyr318Ter**	**2 (0.3)**	**0 (0)**	**0.04**	**NC**	**NC**	**0**	**0**
9	c.1010T>C	p.Val337Ala	0 (0)	1 (0.04)	1.0	–	–	63	90
Intron 9	**c.1072+1G>T**	**p.Asp330fs[a]**	**0 (0)**	**1 (0.04)**	**1.0**	**–**	**–**	**0**	**0**
Intron 9	**c.1073-2A>G**	**p.Tyr358fs[a]**	**1 (0.2)**	**0 (0)**	**0.2**	**–**	**–**	**0**	**0**
10	c.1115G>A	p.Gly372Asp	1[c] (0.2)	0 (0)	0.2	–	–	25	34
10	c.1203G>C	p.Lys401Asn	1 (0.2)	0 (0)	0.2	–	–	115	103
10	**c.1217C>T**	**p.Ala406Val**	**1 (0.2)**	**0 (0)**	**0.2**	**–**	**–**	**0**	**87**
All variants with apparent activity <20%			**8 (1.3)**	**9 (0.4)**	**0.01**	**3.6**	**1.4–9.5**	**–**	**–**

P values were determined by Fisher's exact test. Apparent CPA1 activity and secretion levels were measured as described in **Table 1** and are expressed as a percentage of the wild-type values. Alterations in bold indicate variants with less than 20% apparent activity.
[a]The functional effects of the splice-site variants c.148-1G>A, c.1072+1G>T and c.1073-2A>G were modeled as skipping of exon 3, skipping of exon 9 and retention of intron 9, respectively (as described in the **Supplementary Note**). [b]One individual was homozygous for p.Ala208Thr. [c]This individual was homozygous for this variant. NC, not calculated, as the variant was not detected in controls, rendering the OR infinite.

homozygous for a defective *CPA1* variant. Variants located in noncoding regions and synonymous variants located in coding regions are listed in **Supplementary Table 1**.

We observed that cases bearing a defective *CPA1* variant were younger than those without a *CPA1* alteration. In the German chronic pancreatitis group, the majority of *CPA1* variants with less than 20% apparent activity were present in cases at or below 20 years of age (27/586, 4.6%) (OR = 38.0, 95% CI 14.6–99.1, $P = 6.8 \times 10^{-20}$). This finding was even more significant in a subgroup of cases at or below 10 years of age. In this group, 22/228 (9.7%) carried an impaired *CPA1* variant (OR = 84.0, 95% CI 31.5–224.1, $P = 4.1 \times 10^{-24}$) (cases ≤10 years of age compared to cases ≤20 years of age, $P = 0.007$; cases ≤10 years of age compared to all cases, $P = 7.6 \times 10^{-5}$) (**Table 2**).

We also investigated all *CPA1* exons in 465 German subjects with alcohol-related chronic pancreatitis. Only 2/465 (0.4%) of these individuals were heterozygous for a defective *CPA1* variant: c.954_955delCA (p.Tyr318Ter) in one individual and c.811T>C (p.Cys271Arg) in the other. This indicates that loss-of-function alterations in *CPA1* have a minor role in alcoholic pancreatitis.

To confirm the association of nonalcoholic chronic pancreatitis and *CPA1* in an independent European cohort, we sequenced all *CPA1* exons in 600 cases and 2,432 control subjects originating from France, the Czech Republic and Poland. Again, variants with less than 20% apparent activity were significantly over-represented in chronic pancreatitis cases (8/600, 1.3%) compared to in ethnically matched controls (9/2,432, 0.4%) (OR = 3.6, 95% CI 1.4–9.5, $P = 0.01$) (**Table 3**). One subject with chronic pancreatitis was homozygous for the c.1115G>A (p.Gly372Asp) variant.

To investigate the significance of *CPA1* variants in subjects of non-European descent, we sequenced all ten exons in 230 cases and 264 controls of Indian origin and 247 cases and 341 controls from Japan. Overall, 2.2% (5/230) of the Indian cases but none of the controls

Table 4 Nonsynonymous *CPA1* variants in Indian subjects with nonalcoholic chronic pancreatitis and healthy controls

Exon	Nucleotide change	Amino acid change	Cases (%) (n = 230)	Controls (%) (n = 264)	P	OR	95% CI	Apparent activity	Secretion level
2	c.94G>C	p.Asp32His	1 (0.4)	0 (0)	0.5	–	–	79	75
5	c.506G>A	p.Arg169His	4 (1.7)	0 (0)	0.046	NC	NC	24	23
6	c.622G>A	p.Ala208Thr	6 (2.6)	7 (2.7)	1.0	–	–	81	73
8	**c.922T>C**	**p.Tyr308His**	**5 (2.2)**	**0 (0)**	**0.02**	**NC**	**NC**	**3**	**17**
All variants with apparent activity <20%			**5 (2.2)**	**0 (0)**	**0.02**	**NC**	**NC**	**–**	**–**

P values were determined by Fisher's exact test. Apparent CPA1 activity and secretion levels were measured as described in **Table 1** and are expressed as a percentage of the wild-type values. Alterations in bold indicate variants with less than 20% apparent activity. NC, not calculated, as the variant was not detected in controls, rendering the OR infinite.

Table 5 Nonsynonymous *CPA1* variants in Japanese subjects with nonalcoholic chronic pancreatitis and healthy controls

Exon	Nucleotide change	Amino acid change	Cases (%) (n = 247)	Controls (%) (n = 341)	P	OR	95% CI	Apparent activity	Secretion level
4	c.410C>G	p.Ala137Gly	1 (0.4)	0 (0)	0.42	–	–	52	56
7	**c.713A>T**	**p.Lys238Met**	**1 (0.4)**	**0 (0)**	**0.42**	**–**	**–**	**0**	**3**
7	**c.751G>A**	**p.Val251Met**	**2 (0.8)**	**0 (0)**	**0.18**	**–**	**–**	**0**	**0**
7	**c.764G>T**	**p.Arg255Met**	**1 (0.4)**	**0 (0)**	**0.42**	**–**	**–**	**0**	**86**
9	c.1021G>A	p.Ala341Thr	37 (15.0)	53 (15.5)	1.0	–	–	99	85
10	**c.1079-27_1111dup60**	**p.Thr368_Tyr369ins20[a]**	**1 (0.4)**	**0 (0)**	**0.42**	**–**	**–**	**0**	**49**
All variants with apparent activity <20%			**5 (2.0)**	**0 (0)**	**0.013**	**NC**	**NC**	**–**	**–**

P values were determined by Fisher's exact test. Apparent CPA1 activity and secretion levels were measured as described in **Table 1** and are expressed as a percentage of the wild-type values. Alterations in bold indicate variants with less than 20% apparent activity.
[a]The functional effect of the variant c.1079-27_1111dup60 was modeled as an insertion of 20 amino acids between Thr368 and Tyr369 (as described in the **Supplementary Note**).
NC, not calculated, as the variant was not detected in controls, rendering the OR infinite.

carried a defective *CPA1* variant (P = 0.02) (**Table 4**). In the Japanese sample collection, 2.0% (5/247) of the cases but none of the controls carried an impaired *CPA1* variant (P = 0.013) (**Table 5**). No individual from India or Japan was compound heterozygous or homozygous for a defective *CPA1* variant.

Chronic pancreatitis is a complex multigenic disease, and affected individuals often carry mutations in several disease-associated genes. To elucidate the relationship between *CPA1* alterations and *PRSS1*, *SPINK1*, *CTRC* and *CFTR* variants, we investigated all German subjects with chronic pancreatitis for variants in *PRSS1* (encoding p.Ala16Val, p.Asn29Ile and p.Arg122His), *SPINK1* (encoding p.Asn34Ser and c.194+2T>C), *CTRC* (encoding p.Arg254Trp and p.Lys247_Arg254del) and *CFTR* (encoding p.Phe508del). In total, 50/944 (5.3%) individuals carried a heterozygous *PRSS1* variant, 147/944 (15.6%) were positive for *SPINK1* p.Asn34Ser (121 heterozygotes and 18 homozygotes) and c.194+2T>C (20 heterozygotes, 12 of which were compound heterozygous with p.Asn34Ser), 28/944 (3.0%) were positive for a *CTRC* variant (21 instances of p.Arg254Trp and 7 occurrences of p.Lys247_Arg254del), and 42/944 (4.5%) were positive for *CFTR* p.Phe508del. Together, 273/944 (28.9%) of the cases showed at least one of the above-mentioned genetic alterations, and 24/944 (2.5%) of the cases were *trans* heterozygous. However, only 1/29 (3.6%) cases with a defective *CPA1* variant was *trans* heterozygous; this subject carried the *CPA1* c.1073-2A>G alteration (inherited from the mother) and the *SPINK1* p.Asn34Ser variant (inherited from the father). This suggests a limited interaction of *CPA1* variants with variants in other susceptibility genes and stands in contrast with the high number of *trans* heterozygotes for *SPINK1*, *CTRC* and/or *CFTR* variants, as was described recently[14].

The mechanism by which loss-of-function *CPA1* variants predispose to chronic pancreatitis is not intuitively apparent. We found no detectable effect of CPA1 on trypsinogen activation, trypsin activity or degradation of trypsin and trypsinogen by CTRC (**Supplementary Fig. 2**), indicating that *CPA1* variants do not exert their effect by increasing intrapancreatic trypsin activity. However, the low apparent activity of most of the defective variants was due to markedly reduced secretion (**Tables 1–5** and **Supplementary Figs. 1** and **3**), raising the possibility that CPA1 mutants misfold in the endoplasmic reticulum and cause endoplasmic reticulum stress, as has been demonstrated previously for some PRSS1 and CTRC mutants[15,16]. Indeed, expression of the most frequently found p.Asn256Lys variant in AR42J rat acinar cells resulted in endoplasmic reticulum stress, as evidenced by increased splicing of *Xbp1* and elevated mRNA levels of the chaperones *Hspa5* (encoding BiP) and *Calr* (encoding calreticulin) (**Fig. 1**). Considering that CPA1 is one of the most abundant proteins synthesized by the pancreas, misfolding-induced endoplasmic reticulum stress seems to be a plausible mechanism to explain the clinical effects of heterozygous CPA1 variants.

In summary, loss-of-function *CPA1* variants are strongly associated with nonalcoholic chronic pancreatitis, especially early onset disease. Although there was evidence of heterogeneity in the spectrum of variants present in different populations, the identification of functionally impaired *CPA1* variants in both European and non-European sample collections establishes its global role in the pathogenesis of chronic pancreatitis.

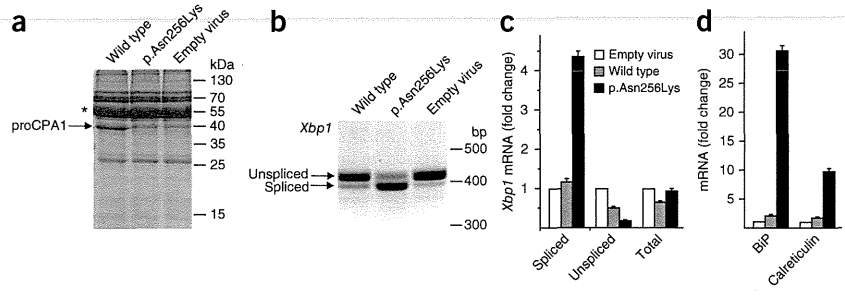

Figure 1 Endoplasmic reticulum stress induced by the p.Asn256Lys CPA1 variant. (**a**) AR42J rat acinar cells were transfected with the indicated wild-type, mutant or empty adenovirus vectors for 24 h using 4 × 10^7 plaque-forming units (pfu) per ml of virus. Conditioned media (200 µl) were precipitated with trichloroacetic acid (10% final concentration) and analyzed by SDS-PAGE and Coomassie blue staining. The p.Asn256Lys mutant had a complete lack of secretion. The faint band at 40 kDa represents an endogenous protein also found in the medium from cells infected with the empty virus. The asterisk indicates the characteristically strong amylase band. See the Online Methods for experimental details. A representative gel of three independent transfections is shown. (**b**) *Xbp1* splicing was assessed by RT-PCR and agarose gel electrophoresis with ethidium bromide staining. A representative gel of three independent experiments is shown. (**c**) Levels of spliced, unspliced and total *Xbp1* mRNA were measured by quantitative real-time PCR and are expressed as fold changes relative to the levels measured in cells transfected with empty adenovirus. (**d**) Quantitative real-time PCR measurements of *Hspa5* (encoding BiP) and *Calr* (encoding calreticulin) mRNA were performed as described in the Online Methods and are expressed as fold changes relative to the levels measured in cells transfected with empty adenovirus. Error bars (**c**,**d**), s.d. (n = 3 independent experiments).

METHODS

Methods and any associated references are available in the online version of the paper.

Accession codes. GenBank: carboxypeptidase A1 (*CPA1*), NT_007933.15 (*Homo sapiens* chromosome 7 genomic contig, GRCh37.p5); NM_001868.2 (human *CPA1* mRNA sequence).

Note: Any Supplementary Information and Source Data files are available in the online version of the paper.

ACKNOWLEDGMENTS

The authors thank all study participants and the members of the Gesellschaft für Pädiatrische Gastroenterologie und Ernährung (GPGE) for providing clinical data and blood samples. The authors also thank C. Ruffert (Leipzig), K. Krohn, K. Schön and B. Oelzner (Interdisziplinäres Zentrum für Klinische Forschung (IZKF) core unit DNA technologies, Leipzig), V. Sahin-Tóth (Boston) and K.R. Mani (CCMB, Hyderabad) for excellent technical assistance. This work was supported by the Deutsche Forschungsgemeinschaft (DFG) grants Wi 2036/2-2 and Wi 2036/2-3 (to H.W.) and RO 3929/1-1 and RO 3939/2-1 (to J.R.), the Else Kröner-Fresenius-Foundation (EKFS) (to H.W.), a grant of the Colora Stiftung gGmbH (to J.R.), US National Institutes of Health (NIH) grants R01DK058088, R01DK082412, R01DK082412-S2 and R01DK095753 (to M.S.-T.), fellowships from the Rosztoczy Foundation (to M. Bence and A. Schnúr), the Bolyai postdoctoral fellowship from the Hungarian Academy of Sciences (to R.S.), INSERM, the Programme Hospitalier de Recherche Clinique (PHRC R 08-04), the French Association des Pancréatites Chroniques Héréditaires and its president N. Meslet, the Czech Ministry of Health conceptual development project of research organization University Hospital Motol in Prague (00064203) and grants CZ.2.16/3.1.00/24022OPPK (to M.M.), the Council of Scientific and Industrial Research (CSIR), Ministry of Science and Technology, Government of India, India grant GENESIS (to G.R.C.), a Grant-in-Aid from the Japan Society for the Promotion of Science (#23591008 to A.M.) and the Research Committee of Intractable Pancreatic Diseases provided by the Ministry of Health, Labour and Welfare of Japan (to A.M. and T.S.).

AUTHOR CONTRIBUTIONS

H.W. and M.S.-T. conceived, designed and directed the study. G.R.C., J.-M.C., J.R., A.M. and H.W. designed, performed and interpreted genetic analyses with substantial contributions from D.B., F.B., M. Braun, S. Bhaskar, C.D., D.L., E.M., S.P., S.S., A.S.-T., K.K., E.N., Y.K., T.S., J.T. and A. Schneider. S. Beer, M. Bence, R.S., A. Szabó, A. Schnúr and M.S.-T. carried out functional characterization of CPA1 variants. H.W., M.S.-T. and S. Beer wrote the manuscript with substantial contributions from G.R.C., J.-M.C., J.R. and A.M. O.L. provided oligonucleotides. All other coauthors recruited study subjects, collected clinical data and provided genomic DNA samples. All authors approved the final manuscript and contributed critical revisions to its intellectual content.

COMPETING FINANCIAL INTERESTS

The authors declare no competing financial interests.

1. Witt, H., Apte, M.V., Keim, V. & Wilson, J.S. Chronic pancreatitis: challenges and advances in pathogenesis, genetics, diagnosis, and therapy. *Gastroenterology* **132**, 1557–1573 (2007).
2. Whitcomb, D.C. *et al.* Hereditary pancreatitis is caused by a mutation in the cationic trypsinogen gene. *Nat. Genet.* **14**, 141–145 (1996).
3. Witt, H., Luck, W. & Becker, M. A signal peptide cleavage site mutation in the cationic trypsinogen gene is strongly associated with chronic pancreatitis. *Gastroenterology* **117**, 7–10 (1999).
4. Le Maréchal, C. *et al.* Hereditary pancreatitis caused by triplication of the trypsinogen locus. *Nat. Genet.* **38**, 1372–1374 (2006).
5. Witt, H. *et al.* Mutations in the gene encoding the serine protease inhibitor, Kazal type 1 are associated with chronic pancreatitis. *Nat. Genet.* **25**, 213–216 (2000).
6. Chandak, G.R. *et al.* Mutations in the pancreatic secretory trypsin inhibitor gene (*PSTI/SPINK1*) rather than the cationic trypsinogen gene (*PRSS1*) are significantly associated with tropical calcific pancreatitis. *J. Med. Genet.* **39**, 347–351 (2002).
7. Rosendahl, J. *et al.* Chymotrypsin C (*CTRC*) variants that diminish activity or secretion are associated with chronic pancreatitis. *Nat. Genet.* **40**, 78–82 (2008).
8. Masson, E., Chen, J.M., Scotet, V., Le Maréchal, C. & Férec, C. Association of rare chymotrypsinogen C (*CTRC*) gene variations in patients with idiopathic chronic pancreatitis. *Hum. Genet.* **123**, 83–91 (2008).
9. Witt, H. *et al.* A degradation-sensitive anionic trypsinogen (*PRSS2*) variant protects against chronic pancreatitis. *Nat. Genet.* **38**, 668–673 (2006).
10. Whitcomb, D.C. *et al.* Common genetic variants in the *CLDN2* and *PRSS1-PRSS2* loci alter risk for alcohol-related and sporadic pancreatitis. *Nat. Genet.* **44**, 1349–1354 (2012).
11. Vendrell, J., Querol, E. & Avilés, F.X. Metallocarboxypeptidases and their protein inhibitors. Structure, function and biomedical properties. *Biochim. Biophys. Acta* **1477**, 284–298 (2000).
12. Szmola, R. *et al.* Chymotrypsin C is a co-activator of human pancreatic procarboxypeptidases A1 and A2. *J. Biol. Chem.* **286**, 1819–1827 (2011).
13. Scheele, G., Bartelt, D. & Bieger, W. Characterization of human exocrine pancreatic proteins by two-dimensional isoelectric focusing/sodium dodecyl sulfate gel electrophoresis. *Gastroenterology* **80**, 461–473 (1981).
14. Rosendahl, J. *et al. CFTR, SPINK1, CTRC* and *PRSS1* variants in chronic pancreatitis: is the role of mutated *CFTR* overestimated? *Gut* **62**, 582–592 (2013).
15. Kereszturi, E. *et al.* Hereditary pancreatitis caused by mutation-induced misfolding of human cationic trypsinogen: a novel disease mechanism. *Hum. Mutat.* **30**, 575–582 (2009).
16. Beer, S. *et al.* Comprehensive functional analysis of chymotrypsin C (*CTRC*) variants reveals distinct loss-of-function mechanisms associated with pancreatitis risk. *Gut* doi:10.1136/gutjnl-2012-303090 (1 September 2012).

[1]Else Kröner-Fresenius-Zentrum für Ernährungsmedizin (EKFZ), Technische Universität München (TUM), Freising, Germany. [2]Zentralinstitut für Ernährungs- und Lebensmittelforschung (ZIEL), TUM, Freising, Germany. [3]Department of Pediatrics, Klinikum Rechts der Isar (MRI), TUM, Munich, Germany. [4]Department of Molecular and Cell Biology, Boston University Henry M. Goldman School of Dental Medicine, Boston, Massachusetts, USA. [5]Department for Internal Medicine, Neurology and Dermatology, Division of Gastroenterology, University of Leipzig, Leipzig, Germany. [6]Institut National de la Santé et de la Recherche Médicale (INSERM), U1078, Etablissement Français du Sang (EFS)–Bretagne, Brest, France. [7]Faculté de Médecine et des Sciences de la Santé, Université de Bretagne Occidentale, Brest, France. [8]Centre for Cellular and Molecular Biology (CCMB), Council of Scientific and Industrial Research (CSIR), Hyderabad, India. [9]Division of Gastroenterology, Tohoku University Graduate School of Medicine, Sendai, Miyagi, Japan. [10]2nd Department of Medicine, Semmelweis University, Budapest, Hungary. [11]Department of Gastroenterology, Hepatology and Immunology, The Children's Memorial Health Institute, Warsaw, Poland. [12]Department of Biology and Medical Genetics, University Hospital Motol and 2nd Faculty of Medicine of Charles University Prague, Prague, Czech Republic. [13]Department of Endocrinology, Sanjay Gandhi Postgraduate Institute of Medical Sciences, Lucknow, India. [14]Institute of Transfusion Medicine and Immunology, Medical Faculty Mannheim, Heidelberg University, Mannheim, Germany. [15]MedGen Health Care Centre, Warsaw, Poland. [16]Department of Medical Genetics, Institute of Mother and Child, Warsaw, Poland. [17]Clinic of Obstetrics and Gynecology, Department of Neonatology, University Hospital Motol and 2nd Medical School, Charles University Prague, Prague, Czech Republic. [18]Department of Gastroenterology, Sanjay Gandhi Postgraduate Institute of Medical Sciences, Lucknow, India. [19]Asian Institute of Gastroenterology, Hyderabad, India. [20]Department of Gastroenterology, Medical College Hospital, Calicut, India. [21]Department of Digestive Tract Diseases, Medical University of Lodz, Lodz, Poland. [22]1st Department of Medicine, University of Szeged, Szeged, Hungary. [23]Department of Internal Medicine, Klinikum Döbeln, Döbeln, Germany. [24]Department of Medicine II, Universitätsmedizin Mannheim, Ruprecht-Karls-Universität Heidelberg, Mannheim, Germany. [25]Institute for Occupational Medicine, Goethe-Universität Frankfurt, Frankfurt, Germany. [26]Department for Transplant Medicine, University Hospital Münster, Albert-Schweitzer-Campus 1, Münster, Germany. [27]Department of Surgery, TUM, Munich, Germany. [28]Department of Gastroenterology, TUM, Munich, Germany. [29]TIB MOLBIOL, Berlin, Germany. [30]Department of Neuropediatrics, Charité, Campus Virchow-Klinikum, Berlin, Germany. [31]NeuroCure Clinical Research Center, Charité, Campus Virchow-Klinikum, Berlin, Germany. [32]Department of Pediatrics, Division of Pediatric Pulmonology, Charité, Campus Virchow-Klinikum, Berlin, Germany. [33]Department of Internal Medicine, Division of Hepatology and Gastroenterology, Charité, Campus Virchow-Klinikum, Berlin, Germany. [34]Department of Pediatrics, University of Halle-Wittenberg, Halle (Saale), Germany. [35]Department of Pediatrics, Justus-Liebig-Universität, Gießen, Germany. [36]Department for Internal Medicine, Neurology and Dermatology, Division of Endocrinology, University of Leipzig, Leipzig, Germany. [37]Integriertes Forschungs- und Behandlungszentrum (IFB) Adiposity Diseases, University of Leipzig, Leipzig, Germany. [38]Universitätsklinik für Pädiatrie I, Department für Kinder-und Jugendheilkunde, Medizinische Universität Innsbruck, Innsbruck, Austria. [39]Sektion für Humangenetik, Medizinische Universität Innsbruck, Innsbruck, Austria. [40]Practice for Digestive and Metabolic Diseases, Leipzig, Germany. [41]Department of Surgery, Universitätsklinikum Dresden, Dresden, Germany. [42]Department of Surgery, Otto-von-Guericke University Magdeburg, Magdeburg, Germany. [43]Department of Clinical Science, Intervention and Technology, Karolinska Institutet, Karolinska University Hospital Huddinge, Stockholm, Sweden. [44]These authors contributed equally to this work. Correspondence should be addressed to H.W. (heiko.witt@lrz.tum.de) or M.S.-T. (miklos@bu.edu).